



Secular evolution of co-orbital motion of two exoplanets: semi-analytical investigation

Vladislav Sidorenko¹

Received: 22 February 2024 / Revised: 17 May 2024 / Accepted: 30 May 2024 /

Published online: 13 June 2024

© The Author(s), under exclusive licence to Springer Nature B.V. 2024

Abstract

We consider a system consisting of a star and two planets in co-orbital motion. The masses of the planets are much smaller than the mass of the star. The problem is planar, the motion of all three bodies taking place in a fixed plane. Since the co-orbital motion corresponds to the 1:1 mean motion resonance, it can be studied by methods developed to investigate resonance effects. In this work, we employ one of the semi-analytical methods intended for studying resonance effects—an adiabatic approximation proposed by J. Wisdom. Evolutionary equations are constructed, which describe secular effects in the dynamics of the system. Using them, various scenarios for the behaviour of the system over long time intervals are analysed in detail. For clarity, diagrams are provided illustrating possible variants of secular evolution.

Keywords Three body problem · Co-orbital motion · Averaging method · Adiabatic invariants

1 Introduction

Let us consider the “planetary” version of the general three-body problem: the mass of one of the bodies significantly exceeds the mass of the other two; and these two smaller bodies are moving around the massive body in slightly perturbed Keplerian orbits. Such a version of the three-body problem can be considered as a model of an exoplanetary system comprising a star and two planets. Astronomical discoveries in recent decades have shown that the motion of planets in exoplanetary systems can differ significantly from the motion of the solar-system planets, which are describing concentric nearly circular orbits located approximately in the same plane. In particular, there is reason to expect the emergence of co-orbital motion in some exoplanetary systems — a regime in which two planets are orbiting a host star with approximately the same period (Laughlin and Chambers 2002; Beaugé et al. 2007; Cresswell and Nelson 2009).

The theoretical possibility of co-orbital motion of celestial bodies was established in the 18th century by Euler and Lagrange (Szebehely 1967). In the Solar System, a large number of asteroids are known to be in co-orbital motion with Jupiter (Emery et al. 2015). However,

✉ Vladislav Sidorenko
vvsidorenko@list.ru

¹ Keldysh Institute of Applied Mathematics, Miusskaya Square 4, Moscow, Russia 125047

a situation when two celestial bodies of comparable masses are in co-orbital motion has so far been observed only in satellite systems of giant planets (Yoder et al. 1989).

A comprehensive review of studies of co-orbital motion in the planetary version of the three-body problem is given in (Tan et al. 2022). The most detailed analysis of the properties of co-orbital motion was probably carried out by Giuppone et al. (2010) and Leleu et al. (2018). In particular, Giuppone et al. (2010) and Leleu et al. (2018) paid special attention to the so-called anti-Lagrangian modes of co-orbital motion, which differ from classical Lagrangian solutions primarily in the orientation of periastrons (see also Hadjidemetriou and Voyatzis 2011).

The study of co-orbital motion in (Giuppone et al. 2010) and (Leleu et al. 2018) was based on selecting some representative initial modes of motion and analysing their subsequent evolution using numerical integration of the equations of motion. The fact that co-orbital motion corresponds to a 1:1 MMR stimulates efforts to obtain additional information about its properties through approaches developed in the theory of resonant effects in Hamiltonian systems. One such approach is the Wisdom adiabatic approximation (Wisdom 1985). An analysis of the secular evolution of co-orbital motion in the adiabatic approximation has already been carried out in (Sidorenko et al. 2014; Sidorenko 2018, 2020), but only in the context of a restricted three-body problem. To study co-orbital motion in the general three-body problem, a number of modifications were required to be introduced into Wisdom's approach.

Wisdom's approach is based on an interpretation of resonance effects given in texts on the modern theory of Hamiltonian systems, see for example Arnold et al. (2006). The behaviour of the system at MMR is characterised by dynamical processes over three time scales: "fast", "semi-fast", and "slow". A "fast" dynamical process is the orbital motion of resonant bodies. A "semi-fast" process is a variation of the resonant phase (a combination of average longitudes and some of the osculating elements of bodies). The "slow" dynamics comprises secular evolution of the shapes and orientation of orbits.

It is worth noting that Wisdom's approach is most efficient in situations where it is sufficient to consider the behaviour of two slow variables to characterise secular effects. If this is the case, then the secular effects can be quite clearly described by drawing evolutionary diagrams. In the general three-body problem, such a simplification is possible when the motion of all bodies occurs in a fixed plane Π of a constant orientation. (Specifically, if the barycentre of the system is at rest, the plane Π is fixed.) Further, when studying co-orbital dynamics, we shall limit our consideration to this case only. Since Giuppone et al. (2010) and Leleu et al. (2018) also concentrated their attention on planar co-orbital motions in the planetary version of the general three-body problem, we hope that our investigation will be a useful complement to these studies. The approach we apply allows us to establish properties of motion that could not be studied by the methods used by Giuppone et al. (2010) and Leleu et al. (2018) (e.g. quasi-probabilistic transformation of co-orbital motion modes).

Here is a brief description of our research. In Sect. 2, we derive the equations of motion in the planar three-body problem in a form convenient for the application of perturbation technique. In Sect. 3, using a double averaging (over orbital motion and over the variation of the resonant phase), the evolutionary equations are constructed that describe secular effects in co-orbital motion. In Sect. 4, these equations are applied to study the evolution of co-orbital motion when the masses of the planets are equal. To understand the influence of differences in the masses of planets on the evolution of motion, in Sect. 5, as an example, we consider the dynamics of the system in the case when one planet is twice as massive as the other. Section 6 establishes a connection between the characteristics of anti-Lagrangian solutions, and an important parameter of co-orbital motions — the deficit of angular momentum. Section 7

concerns with quasi-probabilistic transformations of co-orbital motion modes. The extent to which the model used and the results obtained relate to the possible co-orbital dynamics in real exoplanetary systems is briefly discussed in Sect. 8. The paper concludes with Sect. 9, which lists the main results and indicates the possible directions for further research. In Appendices A and B, for small values of the angular momentum deficit of the system, approximate formulae are derived for some quantities that determine the qualitative properties of motion.

2 Equations of motion

To write down the equations of motion, we introduce a non-inertial astrocetric reference frame, the axes of which maintain constant directions in the absolute space. We denote the radius vectors of the planets relative to the star as \mathbf{r}_1 and \mathbf{r}_2 . The units of measurement are taken in such a way that the gravitational constant and the total mass of the system are equal to 1. The total mass of the planets will be denoted with μ ; in what follows, μ is treated as a small parameter of the problem. The masses of the planets are equal $\mu\bar{\mu}_1$ and $\mu\bar{\mu}_2$, respectively (it is implied that $\bar{\mu}_1 + \bar{\mu}_2 = 1, \bar{\mu}_k > 0$). The semimajor axes of the planets' osculating orbits are assumed to be of order 1.

We start by writing down the equations of motion of planets around a star in the Lagrangian form

$$\frac{d}{dt} \left(\frac{\partial \mathcal{L}}{\partial \dot{\mathbf{r}}_k} \right) - \frac{\partial \mathcal{L}}{\partial \mathbf{r}_k} = 0 \quad (k = 1, 2), \tag{1}$$

where

$$\begin{aligned} \mathcal{L}(\dot{\mathbf{r}}_k, \mathbf{r}_k) &= T(\dot{\mathbf{r}}_k) + U(\mathbf{r}_k), \\ T(\dot{\mathbf{r}}_k) &= \frac{1}{2} \left\{ \mu [\bar{\mu}_1(1 - \mu\bar{\mu}_1)\dot{r}_1^2 + \bar{\mu}_2(1 - \mu\bar{\mu}_2)\dot{r}_2^2] - 2\mu^2\bar{\mu}_1\bar{\mu}_2(\dot{\mathbf{r}}_1, \dot{\mathbf{r}}_2) \right\}, \\ U(\mathbf{r}_k) &= \mu \left[\frac{\bar{\mu}_1(1 - \mu)}{r_1} + \frac{\bar{\mu}_2(1 - \mu)}{r_2} \right] + \frac{\mu^2\bar{\mu}_1\bar{\mu}_2}{|\mathbf{r}_1 - \mathbf{r}_2|}. \end{aligned}$$

After a transition to canonical variables $\mathbf{p}_k = \partial T / \partial \dot{\mathbf{r}}_k, \mathbf{r}_k$, the equations of motion assume the form

$$\frac{\partial \mathbf{p}_k}{dt} = -\frac{\partial \mathcal{H}}{\partial \mathbf{r}_k}, \quad \frac{\partial \mathbf{r}_k}{dt} = \frac{\partial \mathcal{H}}{\partial \mathbf{p}_k}, \quad (k = 1, 2).$$

where

$$\begin{aligned} \mathcal{H}(\mathbf{p}_k, \mathbf{r}_k) &= T(\mathbf{p}_k) - U(\mathbf{r}_k), \\ T(\mathbf{p}_k) &= \frac{1}{2} \left[\frac{1}{\mu} \left(\frac{p_1^2}{\bar{\mu}_1} + \frac{p_2^2}{\bar{\mu}_2} \right) + \frac{1}{1 - \mu} (\mathbf{p}_1 + \mathbf{p}_2, \mathbf{p}_1 + \mathbf{p}_2) \right]. \end{aligned}$$

It can be shown that \mathbf{p}_1 and \mathbf{p}_2 are equal to the momenta of the planets in an inertial coordinate system, with the origin in the barycentre (Laskar and Robutel 1995; Morbidelli 2002).

Following Robutel et al. (2016), we introduce ‘‘scaled’’ impulses $\bar{\mathbf{p}}_k = \mathbf{p}_k / \mu$ to remove a singularity in the expression for kinetic energy at $\mu \rightarrow 0$. The change in variables

$$(\mathbf{p}_k, \mathbf{r}_k) \mapsto (\bar{\mathbf{p}}_k, \mathbf{r}_k)$$

is a canonical transformation with the valency μ^{-1} . After this transformation the Hamiltonian of the system takes the form

$$\tilde{\mathcal{H}}(\bar{\mathbf{p}}_k, \mathbf{r}_k) = \tilde{\mathcal{H}}_0(\bar{\mathbf{p}}_k, \mathbf{r}_k) - \mu V(\bar{\mathbf{p}}_k, \mathbf{r}_k) + O(\mu^2),$$

where

$$\begin{aligned} \tilde{\mathcal{H}}_0(\bar{\mathbf{p}}_k, \mathbf{r}_k) &= \tilde{\mathcal{H}}_{01}(\bar{\mathbf{p}}_1, \mathbf{r}_1) + \tilde{\mathcal{H}}_{02}(\bar{\mathbf{p}}_2, \mathbf{r}_2), \quad \tilde{\mathcal{H}}_{0k}(\bar{\mathbf{p}}_k, \mathbf{r}_k) = \frac{\bar{p}_k^2}{2\bar{\mu}_k} - \frac{\bar{\mu}_k}{r_k} \quad (k = 1, 2), \\ V(\bar{\mathbf{p}}_k, \mathbf{r}_k) &= \frac{\bar{\mu}_1\bar{\mu}_2}{|\mathbf{r}_1 - \mathbf{r}_2|} - \frac{\bar{\mu}_1}{r_1} - \frac{\bar{\mu}_2}{r_2} - \frac{1}{2}(\bar{\mathbf{p}}_1 + \bar{\mathbf{p}}_2, \bar{\mathbf{p}}_1 + \bar{\mathbf{p}}_2). \end{aligned}$$

We observe that $\tilde{\mathcal{H}}_{0k}(\bar{\mathbf{p}}_k, \mathbf{r}_k)$ is the Hamiltonian of an integrable system describing the motion of an object of mass $\bar{\mu}_k$ in a field with potential $-\bar{\mu}_k/r_k$. The ‘‘action-angle’’ variables for this system are the well-known Delaunay elements (Morbidelli 2002). Since we are considering the case where the planets do not leave the plane Π in their motion, then to characterise the motion of each planet we need only two pairs of the Delaunay elements (Szebehely 1967, Ch. 7)

$$\begin{aligned} L_k &= \bar{\mu}_k \sqrt{a_k}, \quad l_k, \\ G_k &= L_k \sqrt{1 - e_k^2}, \quad \varpi_k. \end{aligned}$$

Here, a_k, e_k, ϖ_k denote the values of the semimajor axis, eccentricity, and longitude of the periastron of the k -th planet’s orbit in the limiting case of $\mu = 0$ (i.e., in the case where both planets actually become ‘‘test particles’’ moving around a star of unit mass). The difference between the Keplerian elements introduced in this way and the traditionally used osculating elements is of the order of μ , so in a qualitative study of the evolution of motion over long time interval ($\sim \mu^{-1}$) this difference can be neglected.

After the canonical transformation

$$(\bar{\mathbf{p}}_k, \mathbf{r}_k) \mapsto (L_k, G_k, l_k, \varpi_k),$$

the Hamiltonian of the problem can be written as

$$\tilde{\mathcal{H}} = -\frac{\bar{\mu}_1^3}{2L_1^2} - \frac{\bar{\mu}_2^3}{2L_2^2} - \mu V(L_1, L_2, G_1, G_2, l_1, l_2, \varpi_1 - \varpi_2) + O(\mu^2). \tag{2}$$

The arguments of the disturbing function in (2) are written in such a way to emphasise its dependence on the difference in periastron longitudes, not on the value of each of the quantities ϖ_k separately.

Taking the last property into account, it is reasonable to replace variables G_k, ϖ_k with variables

$$P_\Sigma = \frac{1}{2}(G_1 + G_2), P_\Delta = \frac{1}{2}(G_1 - G_2), \varpi_\Sigma = \varpi_1 + \varpi_2, \varpi_\Delta = \varpi_1 - \varpi_2. \tag{3}$$

It is easy to check that formulae (3) define a canonical transformation. The variable P_Σ , conjugate to the cyclic variable ϖ_Σ , is the first integral of the problem. Its value is proportional to the value of the angular momentum of the system relative to the barycentre.

3 Derivation of evolutionary equations

3.1 The region of co-orbital motion in the phase space of the system

In the phase space of the system, the MMR 1:1 is realised in the region defined by the condition

$$|\bar{\mu}_2 L_1 - \bar{\mu}_1 L_2| \lesssim \mu^{1/2}. \tag{4}$$

In this region, $\dot{\lambda}_1 - \dot{\lambda}_2 \sim \mu^{1/2}$, where $\lambda_k = l_k + \varpi_k$ are the planets' mean longitudes.

To study resonant phenomena, it is necessary to make a change in variables, after which one of the phase variables will become the resonant phase

$$\varphi = \lambda_1 - \lambda_2 = l_1 - l_2 + \varpi_\Delta.$$

This procedure can be accomplished in various ways. Below, we shall discuss the circumstances under which one or another option turns out to be preferable. For definiteness, now we introduce φ using the canonical transformation

$$(L_1, L_2, P_\Sigma, P_\Delta, l_1, l_2, \varpi_\Sigma, \varpi_\Delta) \mapsto (\bar{P}_\varphi, \bar{P}_l, \bar{P}_\Sigma, \bar{P}_\Delta, \varphi, l, \varpi_\Sigma, \varpi_\Delta), \tag{5}$$

defined by the generating function

$$S_1 = (l_1 - l_2 + \varpi_\Delta) \bar{P}_\varphi + l_1 \bar{P}_l + \varpi_\Sigma \bar{P}_\Sigma + \varpi_\Delta \bar{P}_\Delta. \tag{6}$$

Under transformation (5), the old and new variables are connected by the relations

$$\bar{P}_\varphi = -L_2, \quad \bar{P}_l = L_1 + L_2, \quad \bar{P}_\Sigma = P_\Sigma, \quad \bar{P}_\Delta = P_\Delta + L_2, \quad l = l_1.$$

In the resonant region (4), the following estimates for the evolution rates of the ‘‘angular’’ variables $l, \varphi, \varpi_\Sigma, \varpi_\Delta$ are valid:

$$\frac{dl}{dt} \sim 1, \quad \frac{d\varphi}{dt} \sim \mu^{1/2}, \quad \frac{d\varpi_\Sigma}{dt} \sim \frac{d\varpi_\Delta}{dt} \sim \mu.$$

The next step in constructing evolutionary equations is averaging the perturbing function V over the fast variable l . The result can be written down as

$$\begin{aligned} \langle V \rangle_l &= \bar{\mu}_1 \bar{\mu}_2 W + \dots, \\ W &= \frac{1}{2\pi} \int_0^{2\pi} \left[\frac{1}{|\mathbf{r}_1(l) - \mathbf{r}_2(l_2(l))|} - (\dot{\mathbf{r}}_1(l), \dot{\mathbf{r}}_2(l_2(l))) \right] dl. \end{aligned} \tag{7}$$

The dots in (7) denote the terms, which depends only on the values of the semimajor axes of the planets' orbits. For the analysis being carried out, these terms are unimportant.

To find the value of W , it is necessary to solve the Kepler equation to determine the position of both planets. It is convenient to replace the integration over l with an integration over the eccentric anomaly E_1 of the first planet. In this case, it will be sufficient to solve the Kepler equation only to determine the position of the second planet:

$$W = \frac{1}{2\pi} \int_0^{2\pi} \left[\frac{1}{|\mathbf{r}_1(E_1) - \mathbf{r}_2(l_2(E_1))|} - (\dot{\mathbf{r}}_1(E_1), \dot{\mathbf{r}}_2(l_2(E_1))) \right] (1 - e_1 \cos E_1) dE_1, \tag{8}$$

where

$$l_2(E_1) = (E_1 - e_1 \sin E_1) - \varphi + \varpi_\Delta.$$

Since Hamiltonian (2) is the first integral of the problem, then in the case of a weakly perturbed Keplerian motion of the planets (i.e. in the absence of their close approaches), we have:

$$\frac{\bar{\mu}_1^3}{L_1^2} + \frac{\bar{\mu}_2^3}{L_2^2} \approx const.$$

After averaging, $\bar{P}_l = L_1 + L_2$ will also become a first integral. Given the two restrictions on the possible values of L_k , we conclude that in the cases, where the equations of motion averaged over l describe correctly the dynamics of the system, there is no secular evolution of the variables L_k . Respectively, the change in the values of the semimajor axes of the planets' orbits is reduced to small oscillations around $a = \bar{P}_l^2$.

If the eccentricity of the second planet exceeds the eccentricity of the first planet, then to speed up the solution of the Kepler equation, one can calculate W using the formula

$$W = \frac{1}{2\pi} \int_0^{2\pi} \left[\frac{1}{|\mathbf{r}_1(l_1(E_2)) - \mathbf{r}_2(E_2)|} - (\dot{\mathbf{r}}_1(l_1(E_2)), \dot{\mathbf{r}}_2(E_2)) \right] (1 - e_2 \cos E_2) dE_2,$$

where

$$l_1(E_2) = (E_2 - e_2 \sin E_2) + \varphi - \varpi_\Delta.$$

To do this, the resonant phase should be introduced by a canonical transformation of variables, with the generating function

$$S_2 = (l_1 - l_2 + \varpi_\Delta) \bar{P}_\varphi + l_2 \bar{P}_l + \varpi_\Sigma \bar{P}_\Sigma + \varpi_\Delta \bar{P}_\Delta.$$

In this case, the fast variable is $l = l_2$, so an averaging must be carried out over l_2 (and it becomes possible to proceed to an integration over E_2).

3.2 Intermediate system

When resonant effects in Hamiltonian systems are studied, it is convenient to carry out some rescaling of the variables in the resonance region (4) after an averaging over the fastest processes (Arnold et al. 2006). Instead of t , we take $\tau = \mu^{1/2}t$ as the independent variable. As the variable conjugate to φ , we introduce

$$\Phi = \frac{\bar{P}_\varphi^* - \bar{P}_\varphi}{\mu^{1/2}}.$$

Here $\bar{P}_\varphi^* = -\bar{\mu}_2\sqrt{a}$ is the value of the variable \bar{P}_φ at the exact MMR 1:1 in the limiting case $\mu = 0$.

After standard transformations detailed in Arnold et al. (2006), we obtain the following system describing the evolution of the phase φ and the slow variables $\bar{P}_\Delta, \varpi_\Delta$ in the resonant zone (4):

$$\begin{aligned} \frac{d\Phi}{d\tau} &= -\bar{\mu}_1\bar{\mu}_2 \frac{\partial W}{\partial \varphi}, & \frac{d\varphi}{d\tau} &= \frac{3\Phi}{\bar{\mu}_1\bar{\mu}_2\bar{P}_l^4}, \\ \frac{d\bar{P}_\Delta}{d\tau} &= \varepsilon\bar{\mu}_1\bar{\mu}_2 \frac{\partial W}{\partial \varpi_\Delta}, & \frac{d\varpi_\Delta}{d\tau} &= -\varepsilon\bar{\mu}_1\bar{\mu}_2 \frac{\partial W}{\partial \bar{P}_\Delta}, \end{aligned} \tag{9}$$

where $\varepsilon = \mu^{1/2}$.

One more scaling transformation,

$$\tilde{\Phi} = \frac{\Phi}{\bar{\mu}_1 \bar{\mu}_2 \bar{P}_l}, \quad \tilde{P}_\Sigma = \frac{\bar{P}_\Sigma}{\bar{P}_l}, \quad \tilde{P}_\Delta = \frac{\bar{P}_\Delta}{\bar{P}_l}, \quad \tilde{\tau} = \frac{\tau}{\bar{P}_l^3}, \quad \tilde{\varepsilon} = \bar{\mu}_1 \bar{\mu}_2 \varepsilon, \quad (10)$$

brings Eq. (9) to a more universal form, in which the parameters do not appear explicitly. This rescaling actually reduces the consideration of the co-orbital motion of planets to the case of $a_k \approx 1$.

Note that after all these transformations the averaged equations of motion retain their Hamiltonian form (despite having a non-standard symplectic structure):

$$\begin{aligned} \frac{d\tilde{\Phi}}{d\tilde{\tau}} &= -\frac{\partial \Xi}{\partial \varphi}, & \frac{d\varphi}{d\tilde{\tau}} &= \frac{\partial \Xi}{\partial \tilde{\Phi}}, \\ \frac{d\tilde{P}_\Delta}{d\tilde{\tau}} &= \tilde{\varepsilon} \frac{\partial \Xi}{\partial \varpi_\Delta}, & \frac{d\varpi_\Delta}{d\tilde{\tau}} &= -\tilde{\varepsilon} \frac{\partial \Xi}{\partial \tilde{P}_\Delta}, \end{aligned} \quad (11)$$

where

$$\Xi = \frac{3\tilde{\Phi}^2}{2} + \tilde{W}(\varphi, \varpi_\Delta, \tilde{P}_\Delta, \tilde{P}_\Sigma), \quad \tilde{W}(\varphi, \varpi_\Delta, \tilde{P}_\Delta, \tilde{P}_\Sigma) = \bar{P}_l^2 W(\varphi, \varpi_\Delta, \bar{P}_\Delta, \bar{P}_\Sigma, \bar{P}_l).$$

In the general case, in system (11), the variables $\varpi_\Delta, \tilde{P}_\Delta$ vary much slower than the variables $\varphi, \tilde{\Phi}$. Therefore, in what follows we shall call the first two equations in (11) “the fast subsystem”, while the other two will be called “the slow subsystem”.

The momenta $\tilde{P}_\Sigma, \tilde{P}_\Delta$ and the mean eccentricities e_k of the planets are connected by the relations

$$\bar{\mu}_1 \sqrt{1 - e_1^2} + \bar{\mu}_2 \sqrt{1 - e_2^2} = 2\tilde{P}_\Sigma, \quad \bar{\mu}_1 \sqrt{1 - e_1^2} - \bar{\mu}_2 \sqrt{1 - e_2^2} = 2\tilde{P}_\Delta. \quad (12)$$

Differentiating (12) with respect to $\tilde{\tau}$, we obtain

$$\frac{de_1}{d\tilde{\tau}} = -\frac{\sqrt{1 - e_1^2}}{\bar{\mu}_1 e_1} \frac{d\tilde{P}_\Delta}{d\tilde{\tau}}, \quad \frac{de_2}{d\tilde{\tau}} = \frac{\sqrt{1 - e_2^2}}{\bar{\mu}_2 e_2} \frac{d\tilde{P}_\Delta}{d\tilde{\tau}}. \quad (13)$$

On the other hand, it can be shown that if by substitution $\tilde{P}_\Sigma(e_1, e_2), \tilde{P}_\Delta(e_1, e_2)$ we transform \tilde{W} and $\partial \tilde{W} / \partial \tilde{P}_\Delta$ into the functions with the arguments $\varphi, \varpi_\Delta, e_1, e_2$, then

$$\left. \frac{\partial \tilde{W}}{\partial \tilde{P}_\Delta} \right|_{\tilde{P}_\Sigma = \tilde{P}_\Sigma(e_1, e_2), \tilde{P}_\Delta = \tilde{P}_\Delta(e_1, e_2)} = -\frac{\sqrt{1 - e_1^2}}{\bar{\mu}_1 e_1} \frac{\partial \tilde{W}}{\partial e_1} + \frac{\sqrt{1 - e_2^2}}{\bar{\mu}_2 e_2} \frac{\partial \tilde{W}}{\partial e_2}. \quad (14)$$

From relations (13) and (14), it follows that the equations of the slow subsystem can be written as

$$\begin{aligned} \frac{de_1}{d\tilde{\tau}} &= -\tilde{\varepsilon} \frac{\sqrt{1 - e_1^2}}{\bar{\mu}_1 e_1} \frac{\partial \tilde{W}}{d\varpi_\Delta}, & \frac{de_2}{d\tilde{\tau}} &= \tilde{\varepsilon} \frac{\sqrt{1 - e_2^2}}{\bar{\mu}_2 e_2} \frac{\partial \tilde{W}}{d\varpi_\Delta}, \\ \frac{d\varpi_\Delta}{d\tilde{\tau}} &= \tilde{\varepsilon} \left(\frac{\sqrt{1 - e_1^2}}{\bar{\mu}_1 e_1} \frac{\partial \tilde{W}}{\partial e_1} - \frac{\sqrt{1 - e_2^2}}{\bar{\mu}_2 e_2} \frac{\partial \tilde{W}}{\partial e_2} \right). \end{aligned} \quad (15)$$

Using equations for the slow subsystem in the form (15), we formally increase the dimensionality of the system. It however should be taken into account that the analysis of the planets’ motion will be carried out for fixed values of \tilde{P}_Σ , and will thus be restricted to a

manifold with a certain value of the integral of the angular momentum. On this manifold, the dimension of the phase flow coincides with the dimension of the phase flow of system (11). To parameterise the corresponding integral manifolds, it is convenient to use, instead of \tilde{P}_Σ , the quantity σ given by the formula

$$\sigma = 1 - 2\tilde{P}_\Sigma = 1 - \bar{\mu}_1\sqrt{1 - e_1^2} - \bar{\mu}_2\sqrt{1 - e_2^2}. \tag{16}$$

The quantity σ characterises the angular momentum deficit of the system (Laskar 2017). In other words, it is the difference between the maximal possible value of the angular momentum in co-orbital motion (this maximum corresponding the case of $e_1 = e_2 = 0$) and the angular momentum in the system under study.

Remark. The dependence of the qualitative properties of motion on σ , established below, also remains valid in the case when the condition $a_k \approx 1$ is not satisfied. For this dependence to remain valid, σ must be interpreted as a normalised angular momentum deficit (Chambers 2001; Turrini et al. 2020).

In the process of constructing evolutionary equations, system (11) and its modification, obtained by writing the slow subsystem in the form (15), is an important intermediate stage for us. So it is natural to call this system intermediate.

The solutions of the intermediate system are in some sense reversible: if

$$\varphi(\tilde{\tau}), \tilde{\Phi}(\tilde{\tau}), e_1(\tilde{\tau}), e_2(\tilde{\tau}), \varpi_\Delta(\tilde{\tau})$$

is a solution, then

$$2\pi - \varphi(-\tilde{\tau}), \tilde{\Phi}(-\tilde{\tau}), e_1(-\tilde{\tau}), e_2(-\tilde{\tau}), 2\pi - \varpi_\Delta(-\tilde{\tau})$$

will also be a solution.

3.3 Restrictions on the possible values of planets' eccentricities in co-orbital motion

From the conservation of the total angular momentum, one can find restrictions on the possible values of the eccentricities of exoplanets in motion at a given value of σ . Although the derivation of these restrictions is straightforward, it appears that they have not been written down in previous studies of the co-orbital motion of exoplanets.

Let us assume for definiteness that the mass of the first planet does not exceed the mass of the second planet: $\bar{\mu}_1 \leq \bar{\mu}_2$. If $\sigma \leq \bar{\mu}_1$, then the possible values of the planets' eccentricities e_k satisfy the inequalities

$$e_{k,\min} \leq e_k \leq e_{k,\max}, \tag{17}$$

where

$$e_{k,\min} = 0, \quad e_{k,\max} = \sqrt{1 - \left(1 - \frac{\sigma}{\bar{\mu}_k}\right)^2}, \quad k = 1, 2.$$

In the case of $\bar{\mu}_1 < \sigma \leq \bar{\mu}_2$, we should put in (17)

$$e_{1,\min} = 0, \quad e_{2,\min} = \sqrt{1 - \frac{(1 - \sigma)^2}{\bar{\mu}_2^2}}$$

and

$$e_{1,\max} = 1, \quad e_{2,\max} = \sqrt{1 - \left(1 - \frac{\sigma}{\bar{\mu}_2}\right)^2}.$$

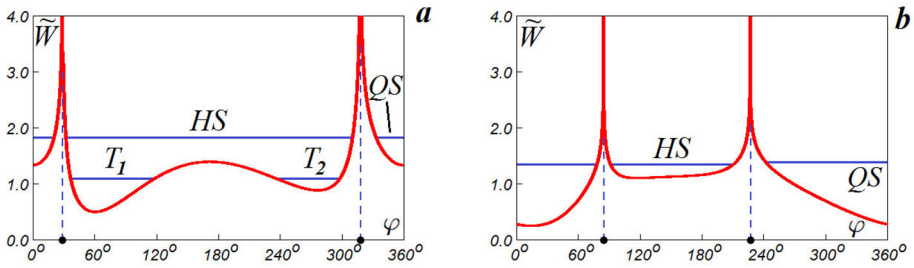


Fig. 1 Behaviour of the function \tilde{W} with fixed ϖ_Δ, e_1, e_2 . Panel **a**: $\varpi_\Delta = 60^\circ, e_1 = e_2 = 0.3$; since there is a local maximum, Trojan modes are possible. Panel **b**: $\varpi_\Delta = 60^\circ, e_1 = 0.9, e_2 = 0.3$; since there is no local maximum, Trojan modes are impossible

Finally, in the case of $\sigma > \bar{\mu}_2$, we set

$$e_{k,\min} = \sqrt{1 - \frac{(1 - \sigma)^2}{\bar{\mu}_k^2}}, \quad e_{k,\max} = 1, \quad k = 1, 2.$$

If we interpret e_k and ϖ_Δ as polar coordinates, then the given formulae allow us to establish the topology of the sets $M_k(\sigma)$ of their possible values for a given σ . If $\sigma \leq \bar{\mu}_1$, then both sets $M_1(\sigma)$ and $M_2(\sigma)$ are discs. In the case of $\bar{\mu}_1 < \sigma \leq \bar{\mu}_2$, the set $M_1(\sigma)$ is a disc, while the set $M_2(\sigma)$ is an annulus. For $\sigma > \bar{\mu}_2$, both sets are annuli.

3.4 Properties of the fast subsystem

Wisdom’s approach involves the averaging of the right-hand sides of the equations for slow variables (15) along the solutions

$$\varphi(\tilde{\tau}, \xi, \varpi_\Delta, e_1, e_2), \quad \tilde{\Phi}(\tilde{\tau}, \xi, \varpi_\Delta, e_1, e_2)$$

of the equations for fast variables

$$\frac{d\varphi}{d\tilde{\tau}} = 3\tilde{\Phi}, \quad \frac{d\tilde{\Phi}}{d\tilde{\tau}} = -\frac{\partial \tilde{W}}{\partial \varphi} \tag{18}$$

in the limit of $\tilde{\varepsilon} = 0$. So let us now take a closer look at this limiting case.

For $\tilde{\varepsilon} = 0$, we are actually dealing with a Hamiltonian system with one degree of freedom. Since in this case the slow variables do not change their values, they play the role of parameters in the Hamiltonian Ξ . The properties of the solutions of (18) are determined by the behaviour of \tilde{W} as a function of the resonant phase φ . Examples of its possible behaviour are shown in Fig. 1. The vertical asymptotes in the given graphs at $\varphi = \varphi_{1,2}(\varpi_\Delta, e_1, e_2)$ correspond to the values of the resonant phase, at which, in the limit of $\varepsilon = 0$, a collision of planets occurs.

If a certain level $\Xi = \xi$ is fixed, then using the given graphs one can establish the number of possible co-orbital motions and draw conclusions about their properties. It should be noted that such analysis was carried out many times within the framework of the restricted three-body problem and a certain terminology has been developed to characterise the possible co-orbital modes in this case: this motion has been termed as a motion in a “quasi-satellite” orbit, or as a motion in a “horseshoe” orbit, or as a motion in one of the two possible “tadpole” orbits, e.g. Namouni et al. (1999), Sidorenko et al. (2014), Sidorenko (2018). Employment of

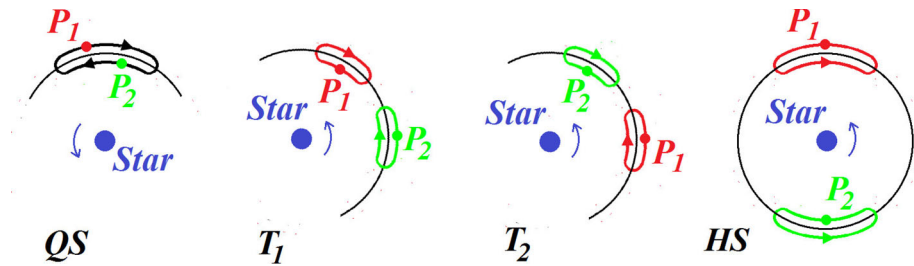


Fig. 2 Different modes of co-orbital motion: *QS*–quasi-satellite mode, T_k –Trojan mode with planet P_k in the lead, *HS*–horseshoe mode. The modes are shown in a reference frame rotating with an angular velocity equal to the averaged value of the planets’ mean motions

the same terminology within the framework of a general problem leads to analogies that are not entirely correct. Therefore, we additionally describe some properties of these motions.

Oscillations of the resonant phase around a value close to zero correspond to a mode that, within the restricted problem, is called “quasi-satellite” (Sidorenko et al. 2014). In the general problem, also, we shall call this mode quasi-satellite, and shall denote it with *QS*. However, for planets of equal mass it is difficult to say which one is a quasi-satellite of the other. Therefore, we may characterise this case as the motion in the mode of a “double” (or “quasi-double”) planet.

“Tadpole” orbits give rise to situations where one of the planets in orbital motion is constantly ahead of the other planet by a certain angle whose value generally evolves with time. Below we shall call such modes “Trojan”, and shall denote them with T_1 or T_2 , depending on which planet is the “leader”.

Our description of the co-orbital modes is closed with the horseshoe mode, denoted as *HS*. In a reference frame rotating with an angular velocity equal to the average of the mean motions of the planets, the relative positions of the planets in the *HS* mode oscillate relative to the position in which they are approximately on opposite sides of the star. The name is due to the fact that the orbit of a less massive planet can actually resemble a horseshoe in the mentioned rotating reference frame. In particular, this always is the case when the values of σ are sufficiently small. By distinction, for sufficiently large values of σ , there is no basis for such an association: planets in the *HS* mode can perform small relative motions.

Figure 2 depicts schematically the listed modes of co-orbital motion.

3.5 Auxiliary functions

Studying the secular evolution of co-orbital motion in the next sections, we fix the value of the Hamiltonian: $\Xi = \xi$. Consequently, the existence of a certain mode of co-orbital motion is determined by how ξ relates to the local and global minima of \tilde{W} as a function of φ . To explore the resulting situations, we introduce several auxiliary functions, similarly to what was done by Neishtadt and Sidorenko (2004), Sidorenko (2018).

The value of the function $H_*(\varpi_\Delta, e_1, e_2)$ is equal to the minimum value of the function $\tilde{W}(\varphi, \varpi_\Delta, e_1, e_2)$ for $\varphi \in (\varphi_1(\varpi_\Delta, e_1, e_2), \varphi_2(\varpi_\Delta, e_1, e_2))$. The value of the function $H^*(\varpi_\Delta, e_1, e_2)$ is equal to the value of the function $\tilde{W}(\varphi, \varpi_\Delta, e_1, e_2)$ in the local maximum (if it exists). If the function $\tilde{W}(\varphi, \varpi_\Delta, e_1, e_2)$ has two local minima in the interval $(\varphi_1(\varpi_\Delta, e_1, e_2), \varphi_2(\varpi_\Delta, e_1, e_2))$, then one minimum is equal to $H_*(\varpi_\Delta, e_1, e_2)$, while the value in the other minimum defines the function $H_{**}(\varpi_\Delta, e_1, e_2)$.

As an example, graphs of the auxiliary functions are presented in Fig. 3 for a system with planets of equal mass, in the case of $\sigma = 0.2$. Since, for a fixed σ , the value of the eccentricity of one planet uniquely sets the value of the eccentricity of the other planet, we actually plotted the graphs of the functions $H_*(\varpi_\Delta, e_1, e_2(e_1, \sigma))$, $H^*(\varpi_\Delta, e_1, e_2(e_1, \sigma))$, $H_{**}(\varpi_\Delta, e_1, e_2(e_1, \sigma))$. Obviously, in the case of equal masses of the planets, these graphs are identical to the graphs of the functions $H_*(\varpi_\Delta, e_1(e_2, \sigma), e_2)$, $H^*(\varpi_\Delta, e_1(e_2, \sigma), e_2)$, $H_{**}(\varpi_\Delta, e_1(e_2, \sigma), e_2)$.

The inequalities $H_*(\varpi_\Delta, e_1, e_2(e_1, \sigma)) < \xi$ and $H_*(\varpi_\Delta, e_1(e_2, \sigma), e_2) < \xi$ define, within the sets $M_1(\sigma)$ and $M_2(\sigma)$ respectively, the forbidden zones onto which the phase trajectories of the intermediate system lying at the level $\Xi = \xi$ cannot be projected.

Level lines $H^*(\varpi_\Delta, e_1, e_2(e_1, \sigma)) = \xi$ and $H^*(\varpi_\Delta, e_1(e_2, \sigma), e_2) = \xi$ set in $M_1(\sigma)$ and $M_2(\sigma)$ so-called uncertainty curves $\Gamma_k(\xi, \sigma)$ (Wisdom 1985; Neishtadt 1987). If $(e_1, \varpi_\Delta) \in \Gamma_1(\xi, \sigma)$ or, the same, if $(e_2, \varpi_\Delta) \in \Gamma_2(\xi, \sigma)$, then a nontrivial solution of the fast subsystem on the level $\Xi = \xi$ in the limiting case $\tilde{\varepsilon} = 0$ is aperiodic. It complicates the use of the averaging method for analysing the secular evolution of co-orbital motions.

Finally, the level lines $H_{**}(\varpi_\Delta, e_1, e_2(e_1, \sigma)) = \xi$ and $H_{**}(\varpi_\Delta, e_1(e_2, \sigma), e_2) = \xi$ define in $M_1(\sigma)$ and $M_2(\sigma)$ the boundaries of regions that differ in the number of possible Trojan modes.

From the example depicted in Fig. 1b, it follows that the functions $H^*(\varpi_\Delta, e_1, e_2)$ and $H_{**}(\varpi_\Delta, e_1, e_2)$ are not defined for all ϖ_Δ, e_1, e_2 . In other words, \tilde{W} as a function of φ does not always have a local maximum and two local minima in the interval $(\varphi_1(\varpi_\Delta, e_1, e_2), \varphi_2(\varpi_\Delta, e_1, e_2))$. A numerical study has revealed that for planets of equal mass at $\sigma \geq \sigma_* \approx 0.202$ there are subsets ϖ_Δ, e_k in $M_k(\sigma)$ in which there are no coexisting Trojan modes for any ξ (Fig. 4). When σ only slightly exceeds σ_* (Fig. 4a), these subsets are small and located in the vicinities of $\varpi_\Delta \approx 41^\circ$ and $\varpi_\Delta \approx 319^\circ, e_k = e_*$, where

$$e_* = \sqrt{1 - (1 - \sigma)^2} \tag{19}$$

As σ increases, the said subsets increase in size (Fig. 4b and c).

The absence of coexisting Trojan modes means that for corresponding values of e_1, e_2, ϖ_Δ only one planet can lead in co-orbital motion with small or moderate amplitude of variation of the resonant phase (in the case when the amplitude of the variation of φ is large enough, the situations $\varphi(\tilde{\tau}) > \pi$ and $\varphi(\tilde{\tau}) < \pi$ will alternate). If the planets are identical, then it would seem that we can replace them in this motion. However, this means replacing $e_1 \rightarrow e_2, e_2 \rightarrow e_1, \varpi_\Delta \rightarrow 2\pi - \varpi_\Delta, \varphi \rightarrow 2\pi - \varphi$ which will give us another solution to the equations of motion.

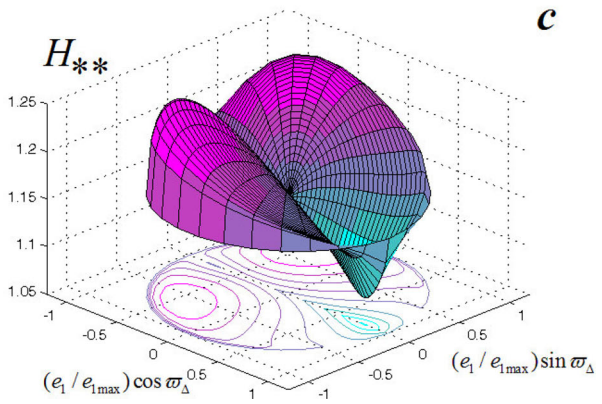
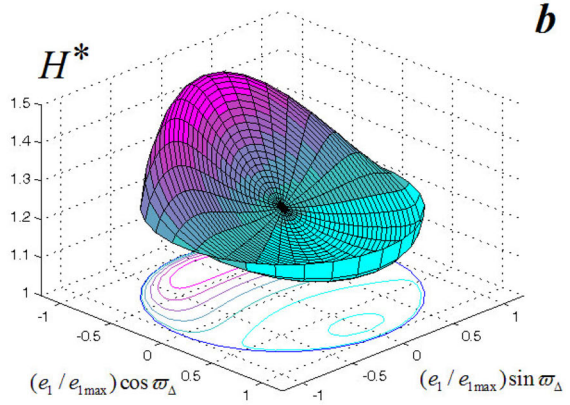
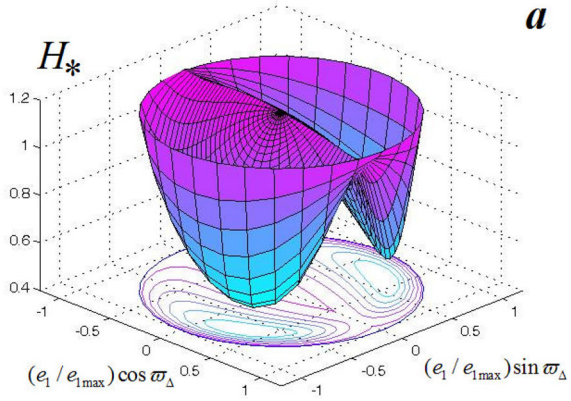
Remark. Using methods significantly different from ours, Leleu et al. (2018) studied how transformations of the set of critical points of the averaged perturbing function at $\sigma = \sigma_*$ affect the properties of co-orbital motion of planets with equal masses.

When exploring the properties of QS motions, it turns out to be convenient to use the function $H_{QS}(\varpi_\Delta, e_1, e_2)$ whose value is equal to the minimum value of $\tilde{W}(\varphi, \varpi_\Delta, e_1, e_2)$ for $\varphi \in (\varphi_2(\varpi_\Delta, e_1, e_2), \varphi_1(\varpi_\Delta, e_1, e_2) + 2\pi)$. In Fig. 5, as an example, a graph of the function H_{QS} is plotted for $\tilde{\mu}_1 = \tilde{\mu}_2 = 0.5, \sigma = 0.2$. The level lines $H_{QS}(\varpi_\Delta, e_1, e_2(e_1, \sigma)) = \xi$ and $H_{QS}(\varpi_\Delta, e_1(e_2, \sigma), e_2) = \xi$ set in $M_1(\sigma)$ and $M_2(\sigma)$, respectively, the boundaries of the regions of existence of the QS modes residing on the level $\Xi = \xi$.

If

$$\varphi = \varpi_\Delta = \psi, \quad e_1 = e_2 = e, \tag{20}$$

Fig. 3 Graphs of auxiliary functions ($\bar{\mu}_1 = \bar{\mu}_2 = 0.5$, $\sigma = 0.2$, $e_{1,2\max} = 0.8$): **a** $H_*(\varpi_\Delta, e_1, e_2(e_1, \sigma))$, **b** $H^*(\varpi_\Delta, e_1, e_2(e_1, \sigma))$, **c** $H_{**}(\varpi_\Delta, e_1, e_2(e_1, \sigma))$



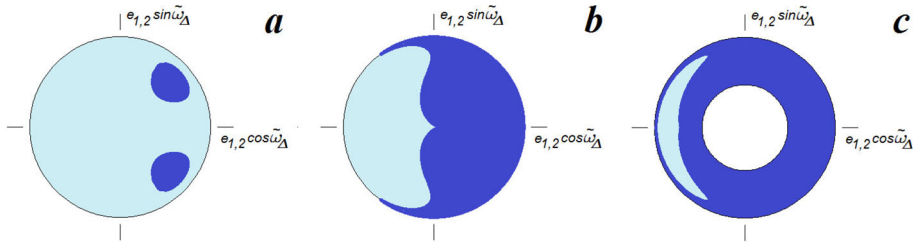


Fig. 4 Subsets of $M_k(\sigma)$ in which a coexistence of Trojan modes is impossible (drawn in deep blue): **a** $\sigma = 0.21$ ($e_{1,2 \max} \approx 0.8146$), **b** $\sigma = 0.29$ ($e_{1,2 \max} \approx 0.9075$), **c** $\sigma = 0.56$ ($e_{1,2 \min} \approx 0.475$, $e_{1,2 \max} = 1$). The planets have equal mass ($\bar{\mu}_1 = \bar{\mu}_2 = 0.5$)

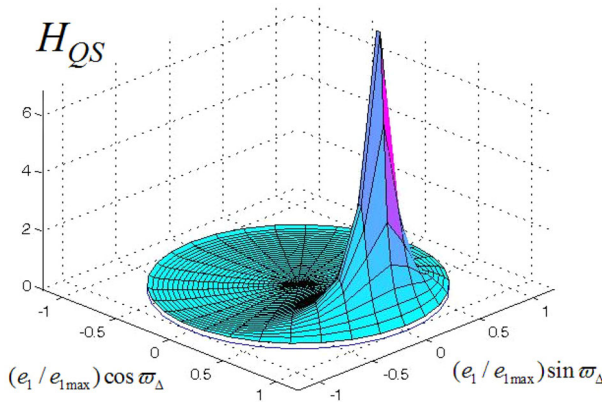


Fig. 5 Graph of the function $H_{QS}(\varpi_\Delta, e_1, e_2(e_1, \sigma))$ for $\bar{\mu}_1 = \bar{\mu}_2 = 0.5$, $\sigma = 0.2$ ($e_{1,2 \max} = 0.8$)

then the value of the function \tilde{W} can be found analytically:

$$\tilde{W} = \frac{1}{2 \sin \frac{\psi}{2}} - \cos \psi.$$

Condition (20) is satisfied in the Lagrangian motions in which the star and planet form an equilateral triangle:

$$\varphi \equiv \frac{\pi}{3}, \quad \varpi_\Delta \equiv \frac{\pi}{3}, \quad e_{1,2} \equiv e,$$

and

$$\varphi \equiv \frac{5\pi}{3}, \quad \varpi_\Delta \equiv \frac{5\pi}{3}, \quad e_{1,2} \equiv e.$$

In this case,

$$\tilde{W}\left(\frac{\pi}{3}, \frac{\pi}{3}, e, e\right) = \tilde{W}\left(\frac{5\pi}{3}, \frac{5\pi}{3}, e, e\right) = \frac{1}{2}.$$

Condition (20) is also satisfied by the Euler solutions, in which the star and the planets are staying permanently on the same straight line:

$$\varphi \equiv \pi, \quad \varpi_\Delta \equiv \pi, \quad e_{1,2} \equiv e.$$

This implies that

$$\tilde{W}(\pi, \pi, e, e) = \frac{3}{2}.$$

The results of the study of the qualitative behaviour of the functions H_* and H^* allow us to conclude that

$$H_*\left(\pi \pm \frac{2\pi}{3}, e, e\right) = W\left(\pi \pm \frac{2\pi}{3}, \pi \pm \frac{2\pi}{3}, e, e\right) = \frac{1}{2}$$

and

$$H^*(\pi, e, e) = W(\pi, \pi, e, e) = \frac{3}{2}.$$

3.6 Evolutionary equations

Now we can perform the last step and write down the evolutionary equations describing the secular effects in the dynamics of the system. To derive these equations, the right-hand sides of the Eq. (15) forming the slow subsystem of the intermediate system must be averaged over the period of oscillation/rotation of the resonant phase φ in the limiting case $\tilde{\varepsilon} = 0$:

$$\begin{aligned} \frac{de_1}{d\tilde{\tau}} &= -\tilde{\varepsilon} \frac{\sqrt{1-e_1^2}}{\bar{\mu}_1 e_1} \left\langle \frac{\partial \tilde{W}}{\partial \varpi_\Delta} \right\rangle, & \frac{de_2}{d\tilde{\tau}} &= \tilde{\varepsilon} \frac{\sqrt{1-e_2^2}}{\bar{\mu}_2 e_2} \left\langle \frac{\partial \tilde{W}}{\partial \varpi_\Delta} \right\rangle, \\ \frac{d\varpi_\Delta}{d\tilde{\tau}} &= \tilde{\varepsilon} \left(\frac{\sqrt{1-e_1^2}}{\bar{\mu}_1 e_1} \left\langle \frac{\partial \tilde{W}}{\partial e_1} \right\rangle - \frac{\sqrt{1-e_2^2}}{\bar{\mu}_2 e_2} \left\langle \frac{\partial \tilde{W}}{\partial e_2} \right\rangle \right). \end{aligned} \tag{21}$$

Here

$$\begin{aligned} \left\langle \frac{\partial \tilde{W}}{\partial \zeta} \right\rangle &= \frac{1}{T(\xi, \varpi_\Delta, e_1, e_2)} \int_0^{T(\xi, \varpi_\Delta, e_1, e_2)} \frac{\partial \tilde{W}}{\partial \zeta}(\varphi(\tilde{\tau}, \xi, \varpi_\Delta, e_1, e_2), \varpi_\Delta, e_1, e_2) d\tilde{\tau}, \\ \zeta &= \varpi_\Delta, e_1, e_2. \end{aligned}$$

Equations (21) have two first integrals. One of them, $\sigma(e_1, e_2) = \text{const}$, is given by relation (16), which follows from the conservation of the angular momentum of orbital motions by the planetary system. The second integral will be the value of the ‘‘action’’ variable of the fast subsystem (an adiabatic invariant of the non-averaged problem, which was found by Wisdom (1985)):

$$J(\xi, \varpi_\Delta, e_1, e_2) = \frac{3\pi}{2} \int_0^{T(\xi, \varpi_\Delta, e_1, e_2)} \tilde{\Phi}^2(\tilde{\tau}, \xi, \varpi_\Delta, e_1, e_2) d\tilde{\tau}.$$

We also note that system (21) ‘‘inherits’’ from the intermediate system the property of reversibility of solutions mentioned in Sect. 3.2. If

$$\varpi_\Delta(\tilde{\tau}), e_1(\tilde{\tau}), e_2(\tilde{\tau})$$

is a solution of (1), then

$$2\pi - \varpi_\Delta(-\tilde{\tau}), e_1(-\tilde{\tau}), e_2(-\tilde{\tau})$$

is a solution of (21).

It is worth noting that if in the process of secular evolution a transition occurs between resonant modes, then it should be taken into account when constructing averaged equations (i.e. averaging should be carried out along the solutions of the subsystem (18), corresponding to these modes). A change in the solution along which averaging is performed occurs when the projection of the phase point $(e_1(\tilde{\tau}), e_2(\tilde{\tau}), \varpi_\Delta(\tilde{\tau}))$ on $M_k(\sigma)$ reaches the uncertainty curve Γ_k . The correctness of the averaging along the solutions that change their qualitative behaviour during evolution is justified in (Neishtadt 1987, 2017).

4 Secular evolution of co-orbital motion in a system with two planets of equal mass

4.1 Preliminary remarks

Evolutionary Eq. (21) are now to be used to study secular effects in the co-orbital motion of the planets. We shall fix different values of the angular momentum deficit σ and different levels $\Xi = \xi$ of the Hamiltonian of the intermediate system. A rather complete picture of the behaviour of solutions on a two-dimensional integral manifold $\sigma(e_1, e_2) = \text{const}$ is given by projections of phase trajectories onto $M_1(\sigma)$ and $M_2(\sigma)$. Similarly to our previous investigations of MMR (Sidorenko et al. 2014; Sidorenko 2018, 2020), we shall pay a special attention to the position of forbidden zones and uncertainty curves Γ_k on the evolutionary diagrams. We shall analyse in great detail the case of equal masses of planets ($\bar{\mu}_1 = \bar{\mu}_2 = 1/2$). In this case, it is reasonable to expect the most significant difference in the properties of motion from what occurs within the framework of the restricted three-body problem.

4.2 Co-orbital motions at small eccentricities ($\sigma \ll 1$)

We open our discussion of the secular effects by considering the QS mode. Without close encounters of the planets (i.e. without their encounters at a distance less than the radius of their Hill spheres), this mode of co-orbital motion cannot be transformed into another mode — nor can it arise as a result of transformation of another mode. Examples of diagrams illustrating the evolution of planetary orbits in the QS mode are shown in Fig. 6. As one can see, in the case of equal masses the diagrams for planet 1 and planet 2 differ only in the direction of the arrows.¹ Therefore, further in this Section we shall present evolutionary diagrams only for one of the two planets.

The evolutionary diagram for quasi-satellite mode is relatively simple: the difference in longitudes of periastrons oscillates around either 0 or π . The only stationary solution corresponds to the anti-apsidal alignment of planetary orbits, with the values of orbital eccentricities in this solution coinciding:

$$\varpi_\Delta = \pi, \quad e_{1,2} = e_* \tag{22}$$

The value of e_* in (22) is provided by formula (19). In particular, if $\sigma = 0.01$, then $e_* \approx 0.14107$.

For $\sigma = 0.01$ the motion of planets in the QS mode becomes possible at $\xi \geq \xi_{QS} \approx 1.4706$ (an approximate expression for ξ_{QS} in the case of $\sigma \ll 1$ is given in Appendix A).

¹ That is to say, if $\varpi_\Delta(\tilde{\tau}), e_1(\tilde{\tau}), e_2(\tilde{\tau})$ is a solution of (21) in the case of $\bar{\mu}_1 = \bar{\mu}_2$, then $2\pi - \varpi_\Delta(\tilde{\tau}), e_2(\tilde{\tau}), e_1(\tilde{\tau})$ will also be a solution.

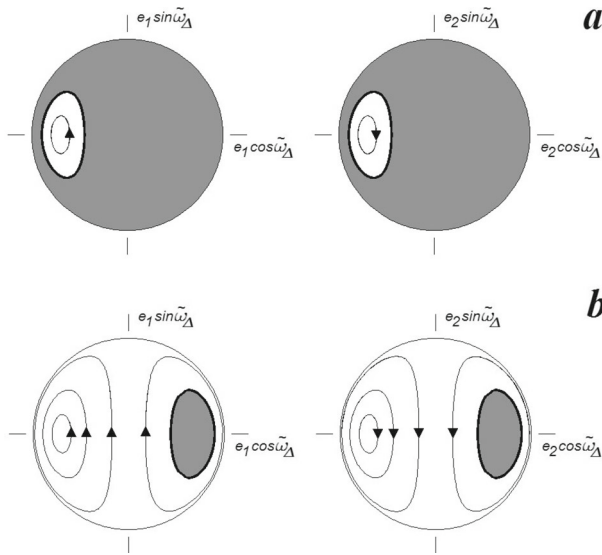


Fig. 6 Evolution of co-orbital motion in the QS mode when the planets have equal masses, $\sigma = 0.01$ and $e_{\max} \approx 0.199$: **a** $\xi = 1.6$, **b** $\xi = 6.5$

The “forbidden” zone (drawn in dark grey) decreases when ξ increases. For large enough ξ , the forbidden zone in $M_k(\sigma)$ is located in a small vicinity of $e_k = e_*$, $\varpi_\Delta = 0$ ($k = 1, 2$).

Figure 7 demonstrates the evolution of other modes of co-orbital motion at $\sigma = 0.01$. The provided examples show the transformation of the structure of evolutionary diagrams with changes in ξ . Green and red tracks correspond to T_1 and T_2 modes. The corresponding evolutionary scenarios differ only in which planet is leading in the orbital motion. The blue tracks correspond to the HS mode, in which the planets are periodically located on the opposite sides of the star.

At $\sigma = 0.01$, the Trojan modes become possible in case $\xi \geq H_*(\frac{\pi}{3}, e_*, e_*) = \frac{1}{2}$ (Fig. 7a). If $\xi = \frac{1}{2}$, then the set of possible values of ϖ_Δ, e_1, e_2 consists of only two elements corresponding to the Lagrange solutions of the three-body problem: $\varpi_\Delta = \frac{\pi}{3}, e_{1,2} = e_*$ and $\varpi_\Delta = \frac{5\pi}{3}, e_{1,2} = e_*$. It is curious that for other σ , and even for other planetary mass ratios, $\frac{1}{2}$ remains the minimum value of ξ at which Trojan modes are possible.

With a further increase in ξ , the areas of Trojan modes increase, and for some values of ϖ_Δ, e_1, e_2 an advanced motion of both the first and second planets becomes possible (Fig. 7b). When the area of coexistence of the Trojan modes increases so much that it includes the motion in which the eccentricity of one of the planets is equal to zero, the evolutionary diagrams assume the form shown in Fig. 7c.

Increasing ξ further, we will observe a decrease of the areas where only one Trojan mode is possible (Fig. 7d) and, finally, a complete disappearance of these areas (Fig. 7e). The disappearance occurs at $\xi \uparrow \xi_{AL} \approx 0.62413$ (where the notation “ \uparrow ” indicates the limit “from the left”). At $\xi = \xi_{AL}$, the “pink” area in the upper part of the evolutionary diagram shrinks into the point $\varpi_\Delta \approx 114.92704^\circ, e_{1,2} = e_*$, while the “green” area in the lower part of the diagram shrinks into the point $\varpi_\Delta \approx 245.07296^\circ, e_{1,2} = e_*$. The critical value ξ_{AL} corresponds to the maximum of the function $H_{**}(\varpi_\Delta, e_1, e_2(e_1, \sigma))$. According to the definition of the function $H_{**}(\varpi_\Delta, e_1, e_2)$, there exists a value φ_{AL} of the resonant phase φ

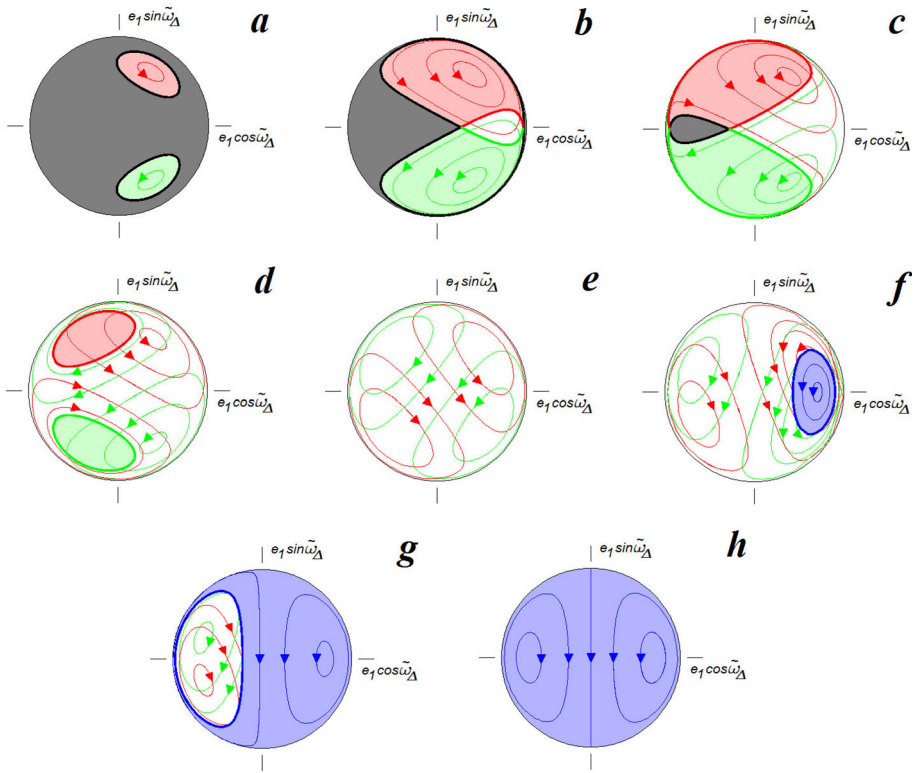


Fig. 7 Evolution of co-orbital motion when the planets have equal masses, $\sigma = 0.01$ and $e_{\max} \approx 0.199$: **a** $\xi = 0.51$, **b** $\xi = 0.55$, **c** $\xi = 0.58$, **d** $\xi = 0.61$, **e** $\xi = 1.10$, **f** $\xi = 1.47$, **g** $\xi = 1.49$, **h** MMR $\xi = 1.70$. Areas in which the only mode of motion is "Trojan" with the leading position of the first planet are drawn in pink. Areas where the only mode is also "Trojan", but the second planet is in the lead, are drawn in green. Areas in which planets move in *HS* mode are drawn in blue

such that

$$\xi_{AL} = \tilde{W}(\varphi_{AL}, \varpi_{\Delta}^{AL}, e_*, e_*), \quad \left. \frac{\partial \tilde{W}}{\partial \varphi} \right|_{\varphi=\varphi_{AL}, \varpi_{\Delta}=\varpi_{\Delta}^{AL}, e_{1,2}=e_*} = 0. \tag{23}$$

The second of relations (23) means that the intermediate system has a stationary solution

$$\varphi \equiv \varphi_{AL}, \quad \tilde{\Phi} \equiv 0, \quad \varpi_{\Delta} \equiv \varpi_{\Delta}^{AL}, \quad e_{1,2} \equiv e_*. \tag{24}$$

The stationary solution (24) can be related to a periodic solution of the non-averaged equations of motion, in which the orbits of the planets precess with an approximately constant values of the following quantities: the resonant phase, the angle between the lines of the apses, and the eccentricities of the orbits. If $\sigma \ll 1$, then in this solution the triangle, whose vertices are the star and the planets, is close to equilateral at any time. The existence of such co-orbital motions was first established by Giuppone et al. (2010). They resemble classical Lagrangian solutions, in which the star and planets form an exact equilateral triangle. Therefore, this mode of motion was called "anti-Lagrangian". More details about "anti-Lagrangian" motions will be provided in Sect. 6.

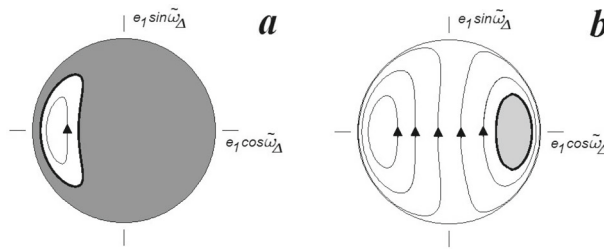


Fig. 8 Evolution of co-orbital motion in QS mode when the planets have equal masses and $\sigma = 0.2$ ($e_{1,2 \max} = 0.8$): **a** $\xi = 1.6$, **b** $\xi = 6.5$

At $\xi = \xi_{HS} \approx 1.4664$, a bifurcation occurs, as a result of which the area of HS motions appears on the evolution diagram (this area is drawn in blue in Fig. 7f). As ξ increases, the area of HS motions increases also (Fig. 7g). At $\xi \uparrow H^*(\pi, e_*, e_*) = \frac{3}{2}$, the area of Trojan modes shrinks to a point. With $\xi > \frac{3}{2}$, only HS motions are possible (Fig. 7h). It is interesting that for $\xi > \frac{3}{2}$, similarly to the case of QS motions for sufficiently large ξ , the difference in the longitudes of periastrons w_Δ oscillates around 0 or π .

Remark. When $\xi \sim \tilde{\epsilon}^{-2} \gg 1$, the variable φ in the solutions of the subsystem (18) actually becomes fast: $d\varphi/d\tilde{\tau} \sim \tilde{\epsilon}^{-1}$. Analysis of the situation when the assumed hierarchy of processes disappears is beyond the scope of our study. The reader can find more information about this in the paper by Robutel and Pousse (2013), where they consider the very extended horseshoe orbits demonstrating the fast variation of φ .

4.3 Co-orbital motions with moderate eccentricities

As a rather representative situation, we consider the case of $\sigma = 0.2$, where the upper border of possible values of the planets' eccentricities is equal to $e_{\max} = 0.8$.

As in Sect. 4.1, we begin our discussion with QS motions. Examples of such motions at $\sigma = 0.2$ are shown in Fig. 8. As in the case of small σ , the region of QS motions arises in the vicinity of the anti-apsidal resonance $e_{1,2} = e_* = 0.6$, $w_\Delta = \Pi$ ($\xi_{QS} \approx 0.045$ for $\sigma = 0.2$). As ξ increases, the region of possible values of the elements of planetary orbits monotonically increases, while the forbidden zone shrinks to the point $e_{1,2} = e_*$, $w_\Delta = 0$.

Examples of the evolution of other modes of co-orbital motion are shown in Fig. 9. Trojan modes appear at $\xi = \frac{1}{2}$ (Fig. 9a). If $\xi \geq \xi_C \approx 1.078$, then for some values of w_Δ , e_1 , e_2 the coexistence of Trojan modes becomes possible (Fig. 9b).

The HS mode becomes possible when $\xi > \xi_{HS} \approx 1.1452$. The appearance of an area where the HS mode takes place occurs before the disappearance of the pink and green areas in which only one Trojan mode is possible (Fig. 9c). This is different from the case of small σ , when this area appeared after the disappearance of areas with only one Trojan mode. In addition, in the case of $\sigma = 0.2$, the stationary solution $w_\Delta \equiv 0$, $e_{1,2} \equiv e_*$ for co-orbital motions in HS mode is unstable.

With a further increase in ξ , we will observe the disappearance of forbidden zones (Fig. 9d).

Transition from the situation shown in Fig. 9e to the situation depicted in Fig. 9f consists of a shrinking and subsequent disappearance of the areas where there is only one Trojan mode. At the bifurcation value $\xi_{AL} \approx 1.2568$ of the parameter ξ , the intermediate system admits a stationary solution, which corresponds to an anti-Lagrangian periodic solution of non-averaged equations of motion.

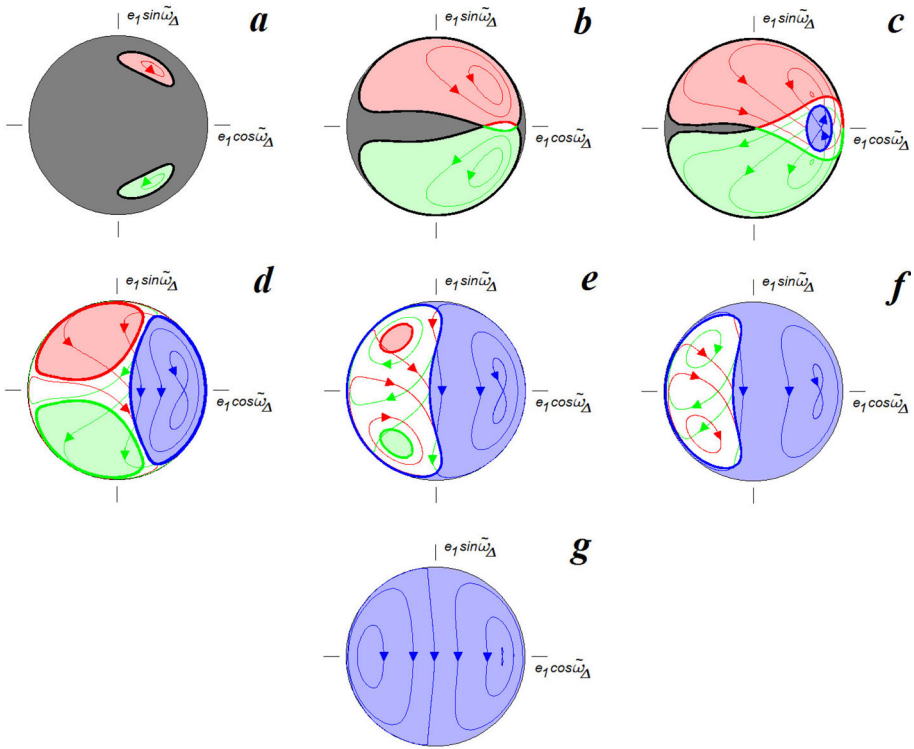


Fig. 9 Evolution of co-orbital motion when the planets have equal masses and $\sigma = 0.2$ ($e_{\max} = 0.8$): **a** $\xi = 0.6$, **b** $\xi = 1.1$, **c** $\xi = 1.15$, **d** $\xi = 1.2$, **e** $\xi = 1.25$, **f** $\xi = 1.3$, **g** $\xi = 1.5$

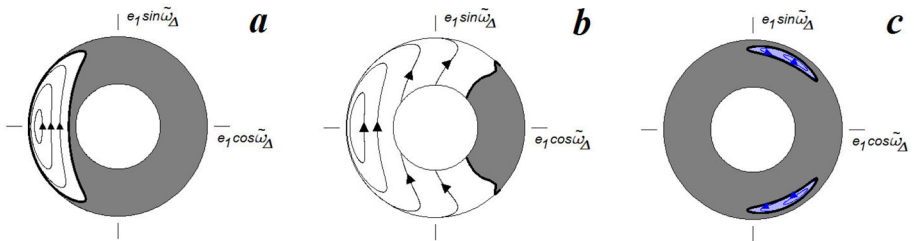


Fig. 10 Evolution of co-orbital motion of planets with equal masses at $\sigma = 0.56$ ($e_{\min} \approx 0.475$, $e_{\max} = 1$). Panes **a** and **b** depict *QS* modes of motion at $\xi = 0.2$ and $\xi = 0.5$, respectively. Pane **c** depicts an *HS* mode at $\xi = 0.7$

At $\xi \geq \frac{3}{2}$, Trojan modes are impossible (Fig. 9g).

4.4 Co-orbital motions with large eccentricities

Figure 10 shows diagrams describing the secular evolution of co-orbital motion at $\sigma = 0.56$. From the formulae given in Sect. refsec3.3, it follows that in this case $e_{1,2} \in [0.475, 1]$. The *QS* mode becomes possible when $\xi \geq \xi_{QS} \approx 0.1451$, see Fig. 10a and b. When $\xi = \frac{3}{2}$, *HS* modes appear, with $\varpi_{\Delta} = \frac{\pi}{3}$, $e_{1,2} = e_*$ and $\varpi_{\Delta} = \frac{5\pi}{3}$, $e_{1,2} = e_*$, where $e_* \approx 0.898$.

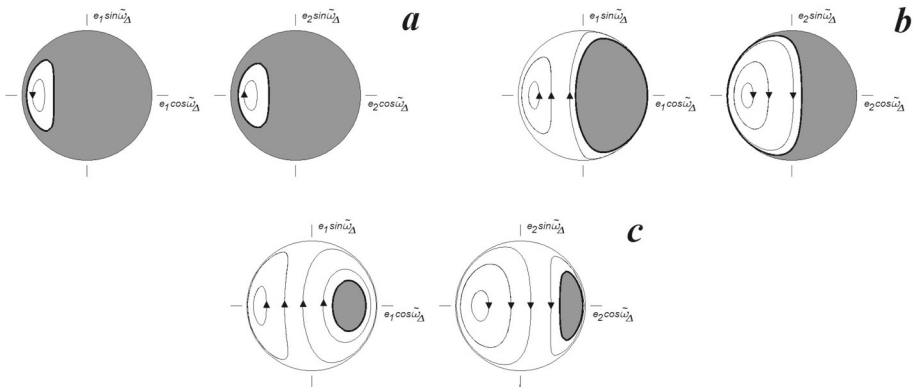


Fig. 11 Evolution of QS modes of co-orbital motion in the case $m_2 = 2m_1, \sigma = 0.1$ ($e_{1\max} \approx 0.714, e_{2\max} \approx 0.527$). Diagram **a, b,** and **c** correspond to the values $\xi = 0.1, \xi = 0.3,$ and $\xi = 1.5,$ respectively

5 Secular evolution of co-orbital motion in the case $m_2 = 2m_1$

We limit our consideration of the co-orbital motion of planets with different masses to the case when the mass of one of the planets is half the mass of the other planet and $\sigma = 0.1$. With these values of the problem parameters, the greatest possible value of the eccentricity of the first planet is $e_{1\max} \approx 0.714$, and the greatest possible value of the eccentricity of the second planet is $e_{2\max} \approx 0.527$.

Figure 11 shows examples of the evolution of quasi-satellite motions at different levels of the Hamiltonian of the intermediate system Ξ . The QS mode is possible in the case when $\xi \geq \xi_{QS} \approx 0.073$. In particular, there is only one QS solution at the level $\Xi = \xi_{QS}$. This is a stationary solution of the intermediate system (15), in which

$$\varphi \equiv 0, \quad \tilde{\Phi} \equiv 0, \quad \varpi_\Delta \equiv \pi, \quad e_1 \approx 0.54, \quad e_2 \approx 0.37. \tag{25}$$

Solution (25) corresponds to anti-apsidal alignment of planetary orbits. If ξ slightly exceeds ξ_{QS} , then in the QS mode at the level $\Xi = \xi$ oscillations of ϖ_Δ around π are observed (Fig. 11a).

Motions with circulation of ϖ_Δ appear at $\xi > \xi_C \approx 0.21$ (Fig. 11b). Finally, at $\xi \geq \xi_R \approx 0.43537$, QS motions with oscillations of ϖ_Δ around 0 (apsidal alignment) become possible (Fig. 11c).

Examples of the evolution of Trojan modes and HS modes are shown in Fig. 12. As in the case of equal masses of planets, Trojan regimes appear at $\xi = \frac{1}{2}$. The value e_* of the eccentricity of planetary orbits in the modes T_k at $\xi = \frac{1}{2}$ can be calculated using formula (19): if $\sigma = 0.1$, then $e_* \approx 0.4359$.

Figure 12a presents an example of evolution in a situation where ξ slightly exceeds $\frac{1}{2}$ (which is the minimal value of ξ that allows the existence of Trojan modes). As ξ increases, the areas of existence of Trojan regimes increase too. When $\xi = \xi_T \approx 0.8202$, the coexistence of Trojan modes T_1 and T_2 becomes possible. In evolutionary diagrams, this corresponds to the appearance of an intersection point at the boundaries of the pink and green areas. The intersection point has coordinates $e_1 \approx 0.34994, \varpi_\Delta = 0$ on the diagram describing the evolution of the motion of the first planet, and coordinates $e_2 \approx 0.47197, \varpi_\Delta = 0$ on the diagram characterising the evolution of the motion of the second planet. Phase portraits for ξ slightly exceeding ξ_T are shown in Fig. 12b.

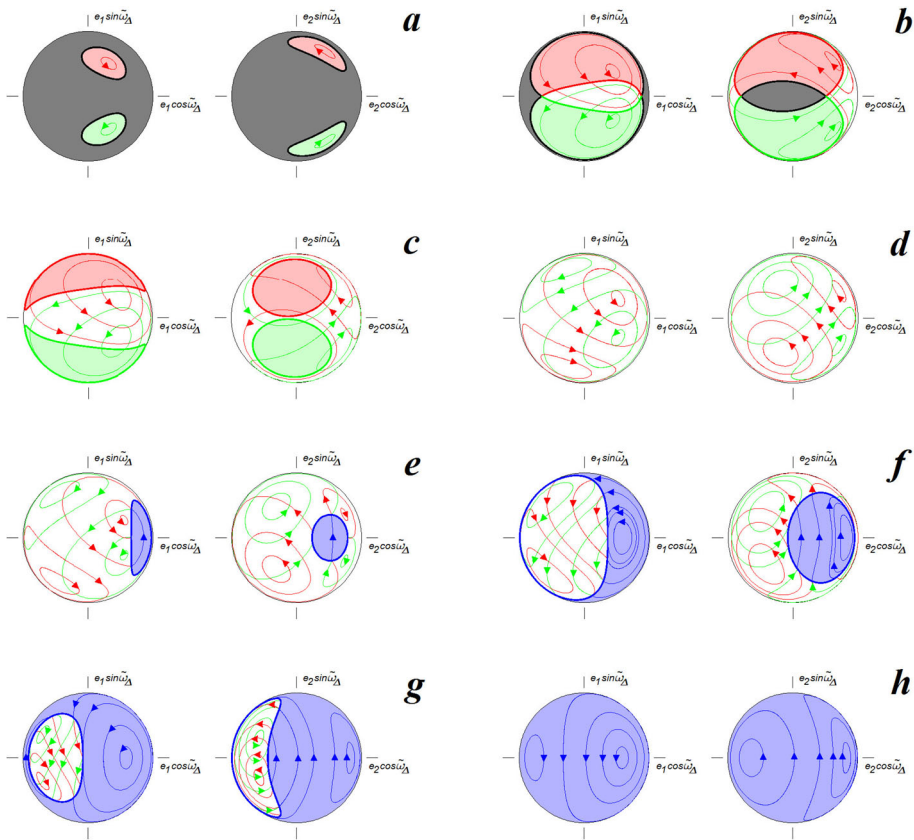


Fig. 12 Evolution of co-orbital motion in the case $m_2 = 2m_1$, $\sigma = 0.1$ ($e_{1 \max} \approx 0.714$, $e_{2 \max} \approx 0.527$): **a** $\xi = 0.6$, **b** $\xi = 1.0$, **c** $\xi = 1.1$, **d** $\xi = 1.2$, **e** $\xi = 1.25$, **f** $\xi = 1.3$, **g** $\xi = 1.4$, **h** $\xi = 1.5$

When $\xi = \xi_F \approx 1.091$, forbidden zones disappear in the evolutionary diagrams. At $\xi \uparrow \xi_{AL} \approx 1.16887$, the areas, in which only one Trojan mode can exist, shrink to the points $e_1 \approx 0.60262$, $\varpi_\Delta \pm 100.62747^\circ$ on the evolutionary diagram of a planet with a smaller mass, and to the points $e_2 \approx 0.30223$, $\varpi_\Delta \pm 100.62747^\circ$ on the evolutionary diagram for a planet with a larger mass. When $\xi = \xi_{HS} \approx 1.23416$, areas of HS motion appear. Examples of evolution diagrams for $\xi \in (\xi_F, \xi_{AL})$, $\xi \in (\xi_{AL}, \xi_{HS})$, and for ξ slightly exceeding ξ_{HS} are provided in Fig. 12c–e, respectively.

Figure 12f and g illustrates the decrease in the area of Trojan modes with a further increase in ξ . When $\xi \uparrow \xi_D = \frac{3}{2}$, this area on evolutionary diagrams shrinks to the point $e_{1,2} = e_*$, $\varpi_\Delta = \pi$. Co-orbital motions at $\xi \geq \xi_D$ are characterised either by circulation ϖ_Δ or its oscillations around 0 or π (Fig. 12h).

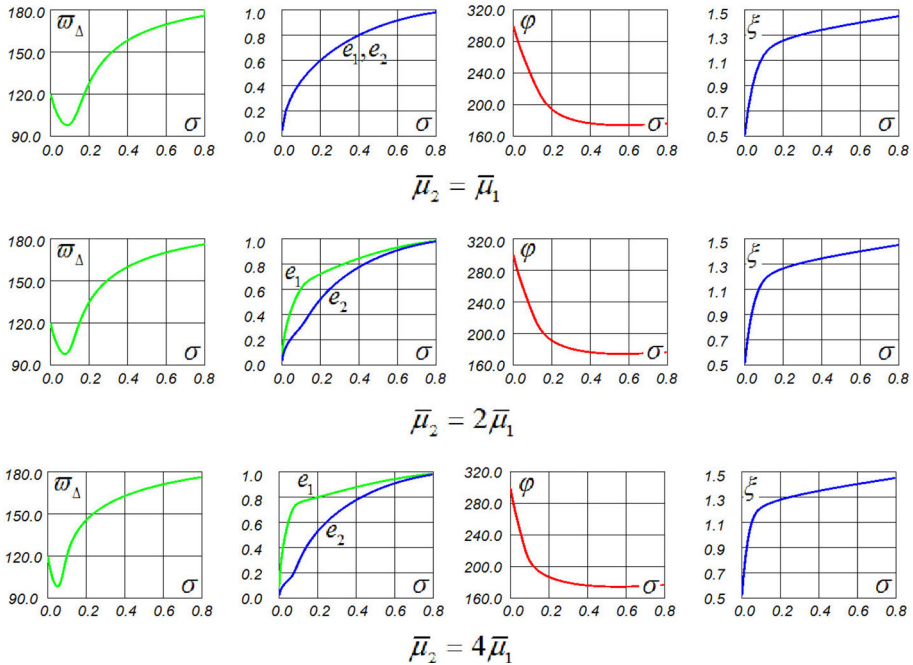


Fig. 13 Characteristics of anti-Lagrangian co-orbital motions at different values of the problem parameters

6 Anti-Lagrangian and anti-Eulerian solutions

The intermediate system introduced in Sect. 3.2 admits two families of stationary solutions. For one of these, the limit $\sigma \rightarrow 0$ implies

$$\varpi_{\Delta} \equiv \varpi_{\Delta}^{AL} \rightarrow \frac{2\pi}{3}, \quad \varphi \equiv \varphi_{AL} \rightarrow \frac{5\pi}{3}. \tag{26}$$

The second family is a symmetrical image of the first one. For those solutions, the limit $\sigma \rightarrow 0$ implies

$$\varpi_{\Delta} \equiv 2\pi - \varpi_{\Delta}^{AL} \rightarrow \frac{4\pi}{3}, \quad \varphi \equiv 2\pi - \varphi_{AL} \rightarrow \frac{\pi}{3}. \tag{27}$$

Solutions (26) and (27) correspond to families of periodic solutions of the non-averaged three-body problem, in which at $\sigma \ll 1$ the star and planets form a rotating triangle close to equilateral (its deviation from equilateral increasing with the increase of σ). From the Lagrangian solutions making an exact equilateral triangle, these solutions also differ in the angle between the lines of apses of the orbits along which the planets move – this can be understood from relations (26) and (27).

The existence of such solutions was first established probably by Giuppone et al. (2010) who were using the averaged Hamiltonian of the three-body problem. They called these solutions anti-Lagrangian. Hadjidemetriou and Voyatzis (2011) obtained anti-Lagrangian solutions numerically for non-averaged motion equations of the three-body problem.

Since our parameterisation of co-orbital motions differs from the parameterisation used in (Giuppone et al. 2010), we had to recalculate some important characteristics of the anti-Lagrangian solutions. Figure 13 shows graphs illustrating the dependence of the properties

of solution (26) on the value of the parameter σ and the planetary mass ratio. Similar graphs for solution (27) can be obtained by obvious symmetry transformations.

The approximate expression for the averaged disturbing function $\tilde{W}(\varphi, \varpi_\Delta, e_1, e_2)$, given in Appendix B, allows us to find the values of the planetary eccentricities in the anti-Lagrangian solutions with $\sigma \ll 1$:

$$e_1 \approx \sqrt{2\sigma \left(\frac{\bar{\mu}_2}{\bar{\mu}_1}\right)}, \quad e_2 \approx \sqrt{2\sigma \left(\frac{\bar{\mu}_1}{\bar{\mu}_2}\right)}. \tag{28}$$

From formulae (28), follows the relation written in (Giuppone et al. 2010) as empirical:

$$\frac{e_1}{e_2} \approx \frac{\bar{\mu}_2}{\bar{\mu}_1}.$$

The intermediate system has also a stationary solution

$$\varphi \equiv \pi, \quad \varpi_\Delta \equiv \pi, \quad e_k \equiv e(\sigma) \quad (k = 1, 2) \tag{29}$$

corresponding to the classical periodic solution of the three-body problem found by Euler (Marchal 1990). In (Leleu et al. 2018), it is noted that solution (29) has an antagonist – an “anti-Eulerian” solution with $\varpi_\Delta \equiv 0$ and $\varphi \equiv \pi$. Using the approximate expression for $\tilde{W}(\varphi, \varpi_\Delta, e_1, e_2)$ from Appendix B, we establish that for $\sigma \ll 1$ the values of eccentricities in the anti-Eulerian solutions also satisfy relations (28).

7 Quasi-probabilistic processes in the vicinity of the uncertainty curve

In the process of constructing evolutionary diagrams, the trajectories of averaged Eq. (23) approaching the uncertainty curve Γ_k and leaving its vicinity were formally “glued”. But a problem arises: on the one side of this curve, we have one solution, while on the other side we have two. Because of this, in some cases we cannot definitely say which mode of motion is realised when the projection of the phase point of the system onto $M_k(\sigma)$ leaves the neighbourhood Γ_k . In phase space, the initial conditions corresponding to different modes of motion after passing Γ_k are strongly mixed. Therefore, the behaviour of the system on the uncertainty curve becomes quasi-probabilistic.

As an example, Fig. 14 shows the results of numerical integration of non-averaged equations, demonstrating how a slight difference in the initial conditions leads to the system’s transition to different modes of motion after passing Γ_k .

Under the scope of a planar restricted three-body problem, quasi-probabilistic transitions between different modes of co-orbital motion were discussed in detail by Sidorenko (2018). In particular, the probabilities of such transitions were calculated. Formulae for calculating the probabilities of transitions between coexisting resonant modes are given in (Artemyev et al. 2013). Similar calculations can be done for the general three-body problem.

8 Applicability of the obtained results to realistic exoplanetary systems

The possibility of co-orbital motions in actual exoplanetary systems has been discussed in the literature heretofore (Laughlin and Chambers 2002; Beaugé et al. 2007; Cresswell and Nelson 2009). Despite intensive efforts to improve the methods for detecting co-orbital motions (see, for example, Giuppone et al. 2012; Leleu et al. 2015), no reliable examples of such motions

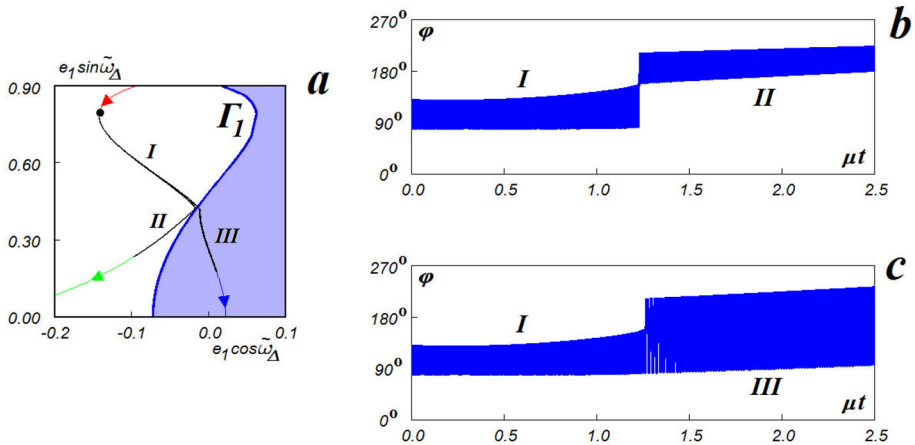


Fig. 14 An example of different behaviour of solutions with close initial data after passing through the neighbourhood of the uncertainty curve. Calculations were carried out for a system with parameters $\bar{\mu}_1 = \bar{\mu}_2$, $\sigma = 0.2$, $\xi = 1.25$, $\mu = 2 \cdot 10^{-6}$. Panel **a** shows the behaviour of slow variables in two solutions of non-averaged equations with initial data that differ in the value of the variable ϖ_Δ by 10^{-5} (black curves). Initially, in both solutions the motion can be described as a Trojan mode with the first planet in the lead. When passing through the neighbourhood of the uncertainty curve, in one solution the Trojan regime is preserved, but the second planet becomes leading. In another solution, the transition to *HS* mode is taking place. Panels **b** and **c** show the change in the behaviour of the resonant phase φ in these solutions (**b** change of the leading planet, **c** motion in *HS* mode)

have been found so far. Nevertheless, the hope that such examples will sooner or later appear is supported by the recent discovery of the formation of dust clumps at one of the triangular libration points of the exoplanet PDS 70b (Balsalobre-Ruza et al. 2023).

As it turned out, good agreement between calculations of secular evolution using Eq. (15) and the results of numerical integration of non-averaged equations of motion is usually achieved at values of the parameter $\mu \sim 10^{-6}$. Thus, if the mass of the star is comparable to the mass of the Sun, then the presented theory of co-orbital motions will be valid for planets with the mass $\sim 10^{-6} m_\odot$. Such planets are classified as “rocky” or “terrestrial”.

9 Concluding remarks

Using the perturbation theory, we have investigated secular effects in the dynamics of a system consisting of a star and two planets in co-orbital motion. For different values of system parameters, evolutionary diagrams have been presented, illustrating changes in motion characteristics over long time intervals.

The analysis was carried out under the scope of a planar three-body problem. Following (Giuppone and Leiva 2016; Robutel and Pousse 2013), it would be interesting to apply our approach to the study of spatial co-orbital motions. It should also be noted that the three-body problem represents a significant simplification of actual dynamics in exoplanetary systems. An important question is, for example, to what extent the results of our analysis of co-orbital motions are applicable to planetary systems having more than two planets (e.g. Couturier et al. 2022; Veras et al. 2016).

Of a particular interest would be taking into account the influence of non-gravitational perturbations on the motion of planets. Non-gravitational perturbations are typically much

weaker than the perturbations caused by the gravitational attraction between the planets. Still, over long time intervals, non-gravitational disturbances can significantly change the motion parameters, which are quasi-integrals for conservative models (for example, the values of semi-major axes).

Non-conservative perturbations of co-orbital motion arise when planets interact with a protoplanetary cloud (Beaugé et al. 2007; Cresswell and Nelson 2009). Another important non-conservative phenomenon is tidal effects (Rodriguez et al. 2013; Couturier et al. 2022). Dobrovolskis and Lissauer (2022) note that tidal friction can lead to destruction of the co-orbital mode of motion.

The adiabatic approximation that we apply to study MMR essentially uses the symplecticity of the phase flow of the three-body problem. However, even in the case when non-conservative perturbations are present, there are no technical obstacles to write down evolutionary equations based on double averaging: over orbital motion and over resonant phase variations.

Appendix A: Approximate formula for calculating the values of the averaged disturbing function in QS mode of co-orbital motion at $\sigma \ll 1$

Using the known series for the coordinates of a celestial body in elliptical motion, we can write down the following approximate formula for the distance between exoplanets in co-orbital motion, valid for small values of the resonant phase φ and small values of eccentricities e_1 and e_2 :

$$\begin{aligned}
 |\mathbf{r}_1 - \mathbf{r}_2|^2 \approx & \varphi^2 + \frac{5}{2} \Lambda(\varpi_\Delta, e_1, e_2) + 4\varphi \Lambda^{1/2}(\varpi_\Delta, e_1, e_2) \sin(\lambda_1 + \hat{\varphi}(\varpi_\Delta, e_1, e_2)) \\
 & - \frac{3}{2} \Lambda(\varpi_\Delta, e_1, e_2) \cos 2(\lambda_1 + \hat{\varphi}(\varpi_\Delta, e_1, e_2)), \tag{A.1}
 \end{aligned}$$

where

$$\begin{aligned}
 \Lambda(\varpi_\Delta, e_1, e_2) &= e_1^2 + e_2^2 - 2e_1e_2 \cos \varpi_\Delta, \\
 \hat{\varphi}(\varpi_\Delta, e_1, e_2) &= -\arccos\left(\frac{e_1 \cos \varpi_\Delta - e_2}{\Lambda^{1/2}}\right) \cdot \text{sign}(\sin \varpi_\Delta).
 \end{aligned}$$

From formula (A.1) it follows that in the case $\sigma \ll 1$ a collision in co-orbital motion is possible under the condition $\varphi = \pm\varphi_* \pmod{2\pi}$, $\varphi_* = 2\Lambda^{1/2}(\varpi_\Delta, e_1, e_2)$. So when exoplanets move in the QS mode, the resonant phase $\varphi \in (-\varphi_*, \varphi_*)$.

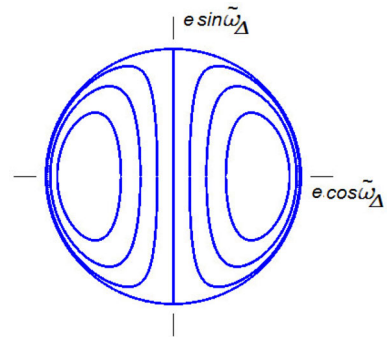
Having formula (A.1), it is easy to obtain an approximate expression for the disturbing function averaged over the orbital motion at 1:1 MMR:

$$\tilde{W}(\varphi, \varpi_\Delta, e_1, e_2) = \frac{1}{\sigma^{1/2}} V\left(\frac{\varphi}{\sigma^{1/2}}, \left(\frac{\Lambda(\varpi_\Delta, e_1, e_2)}{\sigma}\right)^{1/2}\right) + O(1), \tag{A.2}$$

where

$$V(\bar{\varphi}, \kappa) = \frac{1}{2\pi} \int_0^{2\pi} \frac{d\zeta}{\sqrt{\bar{\varphi} + 4\bar{\varphi}\kappa \sin \zeta - \frac{3}{2}\kappa^2 \cos 2\zeta + \frac{5}{2}\kappa^2}}.$$

Fig. 15 Curves on which the projections of phase trajectories lie in the set $M_k(\sigma)$ in the case of QS motion of exoplanets of equal mass. The greatest possible value of eccentricity $e_{\max} = 2\sqrt{\sigma}$



The integral on the right side of the last formula can be reduced to an elliptic one (Byrd and Friedman (1954), formulae (259.00) and (284.00)):

$$V(\bar{\varphi}, \kappa) = \begin{cases} \frac{2}{\pi \sqrt{4\kappa^2 - \bar{\varphi}}} K\left(\sqrt{\frac{3\kappa^2 - \bar{\varphi}^2}{4\kappa^2 - \bar{\varphi}^2}}\right), & |\bar{\varphi}| \leq \sqrt{3}\kappa; \\ \frac{2}{\pi\kappa} K\left(\frac{\sqrt{\bar{\varphi}^2 - 3\kappa^2}}{\kappa}\right), & \sqrt{3}\kappa < |\bar{\varphi}| < 2\kappa. \end{cases}$$

Here $K(\cdot)$ denotes an elliptic integral of the first kind.

From the structure of the expression for the averaged disturbing function (A.2) it follows that the invariance of the value of AI during the secular evolution of co-orbital motion in the QS mode is equivalent to a constant value of the quantity $\Lambda(\varpi_\Delta, e_1, e_2)$. Using the relation $\bar{\mu}_1 e_1^2 + \bar{\mu}_2 e_2^2 \approx 2\sigma$, which is a consequence of (16) at $\sigma \ll 1$, from the condition $\Lambda(\varpi_\Delta, e_1, e_2) = \text{const}$ it is easy to obtain approximate expressions for the projections of phase trajectories on the set $M_1(\sigma)$

$$(\bar{\mu}_2 - \bar{\mu}_1)e_1^2 - 2e_1\bar{\mu}_2^{1/2}\sqrt{2\sigma - \bar{\mu}_1 e_1^2} \cos \varpi_\Delta = \text{const} \tag{A.3}$$

and on the set $M_2(\sigma)$

$$(\bar{\mu}_1 - \bar{\mu}_2)e_2^2 - 2e_2\bar{\mu}_1^{1/2}\sqrt{2\sigma - \bar{\mu}_2 e_2^2} \cos \varpi_\Delta = \text{const}. \tag{A.4}$$

In the case of equal masses of exoplanets, the expressions for the projections of phase trajectories on the sets $M_k(\sigma)$ coincide (Fig. 15):

$$e\sqrt{4\sigma - e^2} \cos \varpi_\Delta = \text{const}, \quad e = e_1, e_2. \tag{A.5}$$

It is obvious that the curves specified by relations (A.3) and (A.4) also define the boundaries of the regions of possible motion of exoplanets in QS mode at a given ξ (cf. Figs. 6 and 15).

Appendix B: Approximate formula for the adiabatic invariant

More specifically, our goal is to derive an approximate formula for calculating the AI values in the HS mode of co-orbital motion at $\sigma \ll 1$. If σ is small enough, then HS motions are possible in the case of

$$\xi > H^*(\varpi_\Delta, e_1, e_2).$$

To calculate the value of the AI for these motions, we employ an approximate formula for the averaged disturbing function:

$$\tilde{W}(\varphi, \varpi_\Delta, e_1, e_2) \approx \tilde{W}_0(\varphi) + \tilde{W}_1(\varphi, \varpi_\Delta, e_1, e_2). \tag{B.1}$$

Here

$$\begin{aligned} \tilde{W}_0(\varphi) &= \frac{1}{\sqrt{2(1 - \cos \varphi)}} - \cos \varphi, \\ \tilde{W}_1(\varphi, \varpi_\Delta, e_1, e_2) &= (e_1^2 + e_2^2)g_1(\varphi) + e_1e_2(\cos \varpi_\Delta \cdot g_2(\varphi) - \sin \varpi_\Delta \cdot g_3(\varphi)), \\ g_1(\varphi) &= \frac{\cos \varphi}{2} + \frac{9 - 5 \cos^2 \varphi - 4 \cos \varphi}{4(2 - 2 \cos \varphi)^{5/2}}, \\ g_2(\varphi) &= 1 - 2 \cos^2 \varphi + \frac{\cos^3 \varphi + 8 \cos^2 \varphi - 5 \cos \varphi - 4}{2(2 - 2 \cos \varphi)^{5/2}}, \\ g_3(\varphi) &= 2 \cos \varphi \sin \varphi + \frac{\sin \varphi(9 - \cos^2 \varphi - 8 \cos \varphi)}{2(2 - 2 \cos \varphi)^{5/2}}. \end{aligned}$$

Formula (B.1) is a slightly modified version of similar formulae presented by Morais (2001) and Sidorenko (2018).

The AI of the considered *HS* motions is given by

$$J(\xi, \varpi_\Delta, e_1, e_2) \approx \frac{1}{2} \int_{\varphi_{\min}(\xi) + \hat{\varphi}_{\min}(\xi, \varpi_\Delta, e_1, e_2)}^{\varphi_{\max}(\xi) + \hat{\varphi}_{\max}(\xi, \varpi_\Delta, e_1, e_2)} \sqrt{\frac{2}{3} [\xi - \tilde{W}_0(\varphi) - \tilde{W}_1(\varphi, \varpi_\Delta, e_1, e_2)]} d\varphi. \tag{B.2}$$

Here $\varphi_{\min}(\xi)$ and $\varphi_{\max}(\xi)$ denote the left and right boundaries of the interval over which the relation $\tilde{W}_0(\varphi) \leq \xi$ is valid. Also, $\hat{\varphi}_{\min}(\xi, \varpi_\Delta, e_1, e_2)$ and $\hat{\varphi}_{\max}(\xi, \varpi_\Delta, e_1, e_2)$ are some small quantities characterising the change in the boundaries of this interval when considering the relation $\tilde{W}_0(\varphi) + \tilde{W}_1(\varphi, \varpi_\Delta, e_1, e_2) \leq \xi$.

Formula (B.2) can be easily reduce to the form

$$J(\xi, \varpi_\Delta, e_1, e_2) \approx J_0(\xi) - d_1(\xi)(e_1^2 + e_2^2) - d_2(\xi)e_1e_2 \cos \varpi_\Delta,$$

where

$$J_0(\xi) = \frac{1}{2} \int_{\varphi_{\min}(\xi)}^{\varphi_{\max}(\xi)} \sqrt{\frac{2}{3} [\xi - \tilde{W}_0(\varphi)]} d\varphi, \quad d_{1,2}(\xi) = \frac{1}{\pi \sqrt{6}} \int_{\varphi_{\min}(\xi)}^{\varphi_{\max}(\xi)} \frac{g_{1,2}(\varphi) d\varphi}{\sqrt{\xi - \tilde{W}_0(\varphi)}}.$$

From the conservation of AI, it follows that, in the course of secular evolution,

$$d_1(\xi)(e_1^2 + e_2^2) + d_2(\xi)e_1e_2 \cos \varpi_\Delta \approx const. \tag{B.3}$$

If the masses of the planets are equal then, at $\sigma \ll 1$, the values of their eccentricities are connected by the relation

$$e_1^2 + e_2^2 \approx 4\sigma. \tag{B.4}$$

From formulae (B.3) and (B.4), we conclude that, during the secular evolution of planets of equal mass,

$$e\sqrt{4\sigma - e^2} \cos \varpi_\Delta \approx const. \tag{B.5}$$

Interestingly, expression (B.5) coincides with the previously obtained expression (A.5), which describes secular effects in the *QS* co-orbital motion.

Acknowledgements The author thanks the anonymous reviewers for helpful comments.

Declarations

Conflict of interest The author declares no conflict of interest.

References

- Arnold, V.I., Kozlov, V.V., Neishtadt, A.I.: *Mathematical Aspects of Classical and Celestial Mechanics*, 3rd edn. Springer, New York (2006)
- Artemyev, A.V., Neishtadt, A.I., Zelenyi, L.M.: Ion motion in the current sheet with sheared magnetic field - Part 1: Quasi-adiabatic theory. *Nonlin. Processes Geophys.* **20**, 163–178 (2013)
- Balsalobre-Ruza, O., de Gregorio-Monsalvo, I., Lillo-Box, J., Huelamo, N., Ribas, A., Benisty, M., Bae, J., Facchini, S., Teague, R.: Tentative co-orbital submillimeter emission within the Lagrangian region L5 of the protoplanet PDS 70b. *Astron. Astrophys.* **675**, A172 (2023)
- Beaugé, C., Sándor, Z., Érdi, B., Süli, Á.: Co-orbital terrestrial planets in exoplanetary systems: a formation scenario. *Astron. Astrophys.* **463**, 359–367 (2007)
- Byrd, P.F., Friedman, M.D.: *Handbook of Elliptic Integrals for Engineers and Physicists*. Springer, Berlin (1954)
- Chambers, J.E.: Making more terrestrial planets. *Icarus* **152**, 205–224 (2001)
- Couturier, J., Robutel, P., Correia, A.C.M.: Dynamics of co-orbital exoplanets in a first-order resonance chain with tidal dissipation. *Astron. Astrophys.* **604**, A1, 19 (2022)
- Cresswell, P., Nelson, R.P.: On the growth and stability of Trojan planets. *Astron. Astrophys.* **493**, 1141–1157 (2009)
- Dobrovolskis, A.R., Lissauer, J.J.: Do tides destabilize Trojan exoplanets? *Icarus* **385**, 115087 (2022)
- Emery, J., Mazari, F., Morbidelli, A., French, L.M., Grav, N.: The complex history of Trojan asteroids. In: Michel, P., et al. (eds), *Asteroids VI* Univ. of Arizona Press, 203–220 (2015)
- Giuppone, C.A., Beaugé, C., Michtchenko, T.A., Ferraz-Mello, S.: Dynamics of two planets in co-orbital motion. *MNRAS* **407**, 390–398 (2010)
- Giuppone, C.A., Benitez-Llambay, P., Beauge, C.: Origin and detectability of co-orbital planets from radial velocity data. *MNRAS* **421**, 356–368 (2012)
- Giuppone, C.A., Leiva, A.M.: Secular models and Kozai resonance for planets in co-orbital non-coplanar motion. *MNRAS* **460**, 966–979 (2016)
- Hadjidemetriou, J.D., Voyatzis, G.: The 1/1 resonance in extrasolar systems. Migration from planetary to satellite orbits. *CMDA* **111**, 178–199 (2011)
- Laskar, J.: Large scale chaos and the spacing of the inner planets. *Astron. Astrophys.* **317**, L75–L78 (2017)
- Laskar, J., Robutel, P.: Stability of the planetary three-body problem. I. Expansion of the Planetary Hamiltonian. *CMDA* **62**, 193–217 (1995)
- Laughlin, G., Chambers, J.E.: Extra-Solar Trojans: the viability and detectability of planets in the 1:1 resonance. *Astrophys. J.* **123**, 592–606 (2002)
- Leleu, A., Robutel, P., Correia, A.C.M.: Detectability of quasi-circular co-orbital planets Application to the radial velocity technique. *Astron. Astrophys.* **581**, A128 (2015)
- Leleu, A., Robutel, P., Correia, A.C.M.: On the coplanar eccentric non-restricted co-orbital dynamics. *CMDA* **130**, 24 (2018)
- Marchal, C.: *The Three-Body Problem*. Elsevier, Amsterdam (1990)
- Morais, M.H.M.: Hamiltonian formulation of the secular theory for Trojan-type motion. *Astron. Astrophys.* **369**, 677–689 (2001)
- Morbidelli, A.: *Modern Celestial Mechanics. Aspects of Solar System Dynamics*. Taylor and Francis, New York (2002)
- Namouni, F., Christou, A.A., Murray, C.D.: Coorbital dynamics at large eccentricity and inclination. *Phys. Rev. Lett.* **83**, 2506–2509 (1999)
- Neishtadt, A.I.: Jumps of the adiabatic invariant on crossing the separatrix and the origin of the 3:1 Kirkwood gap. *Sov. Phys. Dokl.* **32**, 571–573 (1987)
- Neishtadt, A.I.: Averaging method for systems with separatrix crossing. *Nonlinearity* **30**, 2871–2917 (2017)
- Neishtadt, A.I., Sidorenko, V.V.: Wisdom system: dynamics in the adiabatic approximation. *Celest. Mech. Dyn. Astron.* **90**, 307–330 (2004)

- Robutel, P., Niederman, L., Pousse, A.: Rigorous treatment of the averaging process for co-orbital motions in the planetary problem. *Comput. Appl. Math.* **35**, 675–699 (2016)
- Robutel, P., Pousse, A.: On the co-orbital motion of two planets in quasi-circular orbits. *CMDA* **117**, 17–40 (2013)
- Rodriguez, A., Giuppone, C.A., Michtchenko, T.A.: Tidal evolution of close-in exoplanets in co-orbital configurations. *CMDA* **117**, 59–74 (2013)
- Sidorenko, V.V.: Dynamics of “jumping” Trojans: a perturbative treatment. *CMDA* **130**, 1–18 (2018)
- Sidorenko, V.V.: A perturbative treatment of the retrograde co-orbital motion. *Astronomical J.* **160**, 257 (2020)
- Sidorenko, V.V., Neishtadt, A.I., Artemyev, A.V., Zelenyi, L.M.: Quasi-satellite or-bits in the general context of dynamics in the 1: 1 mean motion resonance: perturbative treatment. *CMDA* **120**, 131–162 (2014)
- Szebehely, V.: *Theory of orbits. The restricted problem of three bodies.* Academic Press (1967)
- Tan, P., Shen, X., Hou, X., Liao, X.: A review on co-orbital motion in restricted and planetary three-body problem. *Chinese Astron. Astrophys.* **46**, 346–390 (2022)
- Turrini, D., Zinzi, A., Belinchon, J.A.: Normalized angular momentum deficit: a tool for comparing the violence of the dynamical histories of planetary systems. *Astron. Astrophys.* **636**, A53 (2020)
- Veras, D., Marsh, T.R., Gänsicke, B.T.: Dynamical mass and multiplicity constraints on co-orbital bodies around stars. *MNRAS* **461**, 1413–1420 (2016)
- Yoder, C.F., Synnot, S.P., Salo, H.: Orbits and masses of Saturn’s co-orbiting satellites. Janus and Epimetheus. *Astronomical J.* **98**, 1875–1889 (1989)
- Wisdom, J.: A perturbative treatment of motion near the 3/1 commensurability. *Icarus* **63**, 272–286 (1985)

Publisher’s Note Springer Nature remains neutral with regard to jurisdictional claims in published maps and institutional affiliations.

Springer Nature or its licensor (e.g. a society or other partner) holds exclusive rights to this article under a publishing agreement with the author(s) or other rightsholder(s); author self-archiving of the accepted manuscript version of this article is solely governed by the terms of such publishing agreement and applicable law.